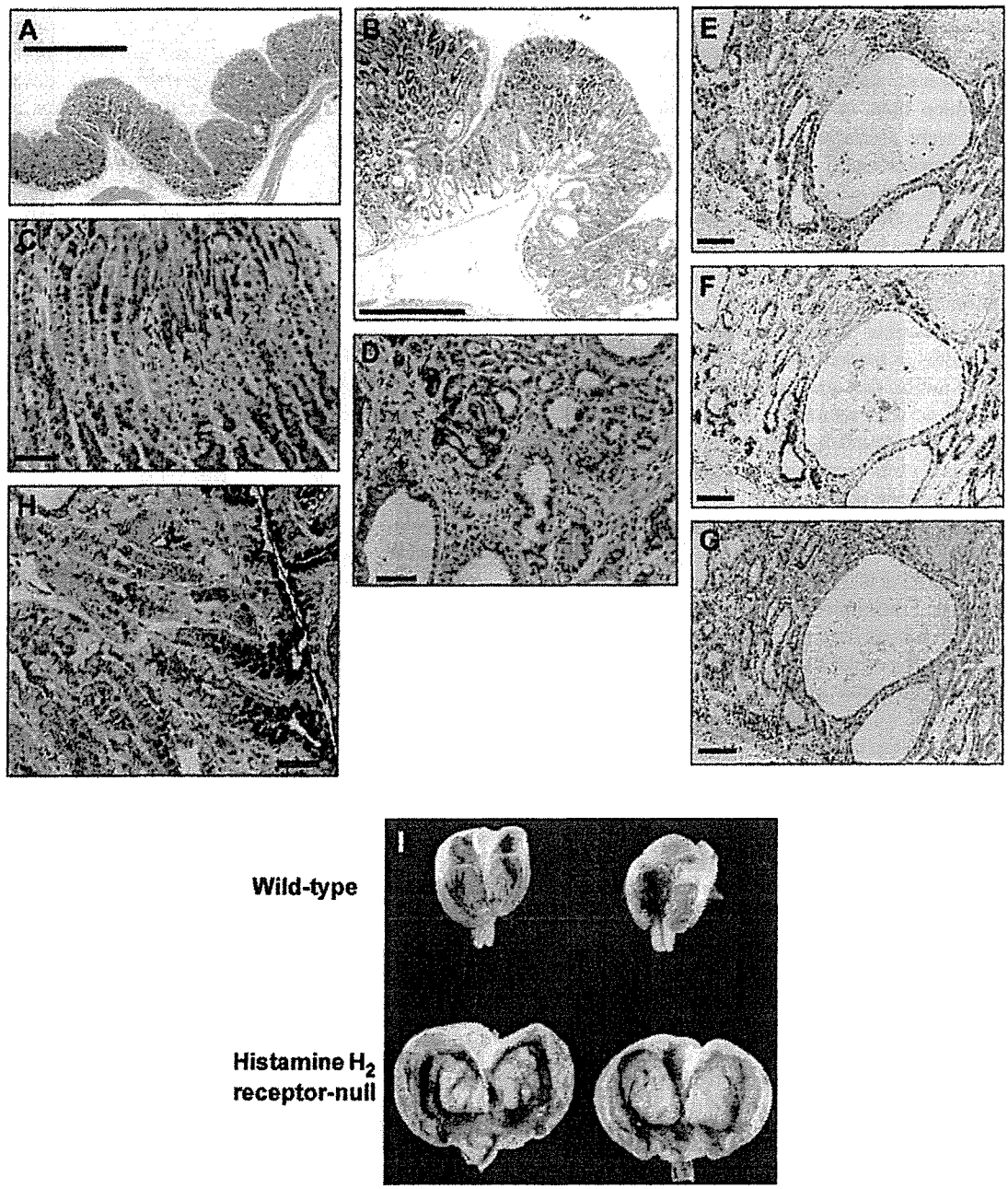

Fig. 7. Oxyntic mucosa from 12-month-old wild-type and histamine H_2 receptor-null mice. A, B, C, D, E, F, G and H Sections of oxyntic mucosa from histamine H_2 receptor-null mice (B, D, E, F, G, H) and wild-type (A, C) mice were stained with hematoxylin and eosin (A, B, C, D) and with anti-$H^{(+)}/K^{(+)}$-ATPase antibody (E), anti-pepsinogen antibody (F) or with anti-HDC antibody (G) and PAS (H). Arrows indicate interstitial cells. Scale bars, 1000 μm (A, B); 100 μm (E, F, G); 50 μm (C, D, H). (I) Macroscopic views of stomachs from wild-type and histamine H_2 receptor-null mice. The excised stomachs from 12-month-old mice were opened along the greater curvature.

that chief cell precursor cells express $H^{(+)}/K^{(+)}$-ATPase (Mutoh et al., 2002). Thus, it is likely that ablation of chief cell precursors rather than ablation of parietal cells resulted in the loss of chief cells observed in the study (Canfield et al., 1996; Li et al., 1996). In contrast, our pepsinogen and type III mucin findings show that the histamine H_2 receptor per se is involved in production and/or secretion of pepsinogen in chief cells. Thus, the histamine H_2 receptor is indispensable for chief cell maturation at least in terms of pepsinogen secretion.

Even in double-null mice, with severely impaired acid production, parietal cells and $H^{(+)}/K^{(+)}$-ATPase were present (Table 1). In addition, electron microscopic analysis of parietal cells from double-null, gastrin receptor-null and histamine H_2 receptor-null mice revealed no essential ultrastructural differences as compared to wild-type mice

(data not shown). Thus, there is no apparent structural alteration in gastric acid secretion mechanisms in double-null mice. However, gastric pH values were higher than in double-null mice than in the other three kinds of mice studied and were unresponsive even to carbachol. In histamine H_2 receptor-null mice, carbachol-induced acid production was mostly preserved (Fukushima et al., 2003; Kobayashi et al., 2000). Thus, considering the loss of the in vivo acid production response in gastrin receptor-null mice, acid production via cholinergic stimuli is largely dependent on the gastrin receptor. The finding that gastrin receptor disruption in histamine H_2 receptor-null mice, i.e. double-null mice, resulted in marked elevation of gastric pH (Fig. 6) reinforces the notion that gastrin receptors in parietal cells function in gastric acid secretion (Fukushima et al., 2003). In any case, it is noteworthy that disrupting histamine H_2 and gastrin receptors resulted in loss of response to secretagogues, even in terms of gastric pH, confirming the pivotal roles of these receptors in gastric acid production and secretion.

Recently, Ogawa et al. (2003) reported that findings in the stomachs of aged histamine H_2 receptor-null mice were compatible with Menetrier's disease. Menetrier's disease is characterized by hyperplasia of oxyntic mucosa which is attributable to hyperplasia of surface mucous cells and is often accompanied by hypoplasia of gland cells and low gastric acidity (Wolfsen et al., 1993; Yamada et al., 1995). As we previously reported, oxyntic mucosa from histamine H_2 receptor-null mice is characterized by marked hyperplasia of downward migrating cells, while hyperplasia of surface mucous cells is negligible (Fukushima et al., 2003). In 12-month-old mice, marked gastric mucosal hypertrophy was observed. However, as shown in Fig. 7, the extremely hypertrophic gastric mucosa consists of markedly elongated glands, cysts which originated from dilated gastric glands and increased interstitial tissues. The contribution of surface mucous cells is minimal. Thus, we consider it difficult to conclude that the gastric mucosal findings of aged histamine H_2 receptor-null mice are compatible with Menetrier's disease.

Rather, histological findings in aged histamine H_2 receptor-null mice can be fully explained by the findings in their 10-week-old counterparts. Oxyntic mucosal stem cells reside in the upper one-third of the mucosa away from the basal region and differentiate, growing upward or downward (Karam and Leblond, 1993a). In histamine H_2 receptor-null mice, marked hyperplasia of downward migrating cells results in unlimited movement of stem cells away from the basal region of the gastric mucosa (Fukushima et al., 2003). In addition, in the mid-portion of gastric glands both the number and mucous content of mucous neck cells are increased, which can lead to increased viscosity of the gastric juice retained in the mid-portions of gastric glands. Thus, due to this marked elongation of gastric glands together with the increased viscosity of gastric juice, gastric glands in histamine H_2 receptor-null mice would presumably be susceptible to occlusion. Once occlusion occurs, secretions from gland cells, even if impaired, promote the formation of cysts. Since gastric pH values per se are essentially preserved in histamine H_2 receptor-null mice (Fukushima et al., 2003; Kobayashi et al., 2000), leakage of contents and cystic rupture are expected to induce inflammation and an increase in interstitial tissues. Therefore, although the phenotype of stomachs from aged histamine H_2 receptor-null mice appears to be quite unusual, there is no essential difference between gastric mucosae from young and aged histamine H_2 receptor-null mice.

In conclusion, we have used double-null mice to show that (1) gastrin and histamine H_2 receptors are both essential in gastric acid production and secretion, (2) the histamine H_2 receptor plays a pivotal role in chief cell maturation, (3) gastrin gene products other than gastrin-17, such as glycine-extended gastrin, might be involved in surface mucous cell proliferation and (4) hypertrophy of gastric mucosa from histamine H_2 receptor-null mice is due to hyperstimulation of gastrin receptors via marked hypergastrinemia. Since gastric oxyntic mucosa is quite unique in that different cell types interact with each other both structurally and functionally, our murine models are potentially valuable for further analyzing differentiation of gastric mucosa and gastric acid secretion mechanisms.

Acknowledgments

This research was supported in part by a grant (to T. Saitoh and T. Ishikawa) from the Ministry of Education, Culture, Sports, Science and Technology, Japan. We are grateful to Ms. Masako Fujita, Ms. Kazuyo Shirai and Ms. Manami Ikematsu for helping with our experiments in this study.

References

Canfield, V., West, A.B., Goldenring, J.R., Levenson, R., 1996. Genetic ablation of parietal cells in transgenic mice: a new model for analyzing cell lineage relationships in the gastric mucosa. Proc. Natl. Acad. Sci. U. S. A. 93, 2431–2435.

Chen, D., Zhao, C.M., Dockray, G.J., Varro, A., Van Hoek, A., Sinclair, N.F., Wang, T.C., Koh, T.J., 2000. Glycine-extended gastrin synergizes with gastrin 17 to stimulate acid secretion in gastrin-deficient mice. Gastroenterology 119, 756–765.

Dockray, G.J., Varro, A., Dimaline, R., Wang, T., 2001. The gastrins: their production and biological activities. Annu. Rev. Physiol. 63, 119–139.

Friis-Hansen, L., Sundler, F., Li, Y., Gillespie, P.J., Saunders, T.L., Greenson, J.K., Owyang, C., Rehfeld, J.F., Samuelson, L.C., 1998. Impaired gastric acid secretion in gastrin-deficient mice. Am. J. Physiol. 274, G561–G568.

Fukushima, Y., Oka, Y., Katagiri, H., Saitoh, T., Asano, T., Ishihara, H., Matsuhashi, N., Kodama, T., Yazaki, Y., Sugano, K., 1993. Desensitization of canine histamine H2 receptor expressed in Chinese hamster ovary cells. Biochem. Biophys. Res. Commun. 190, 1149–1155.

Fukushima, Y., Ohmachi, Y., Asano, T., Nawano, M., Funaki, M., Anai, M., Ogihara, T., Inukai, K., Onishi, Y., Sakoda, H., Saitoh, T., Matsuhashi, N., Yazaki, Y., Sugano, K., 1999. Localization of the histamine H2

receptor, a target for antiulcer drugs, in gastric parietal cells. Digestion 60, 522–527.

Fukushima, Y., Shindo, T., Anai, M., Saitoh, T., Wang, Y., Fujishiro, M., Ohashi, Y., Ogihara, T., Inukai, K., Ono, H., Sakoda, H., Kurihara, Y., Honda, M., Shojima, N., Fukushima, H., Haraikawa-Onishi, Y., Katagiri, H., Shimizu, Y., Ichinose, M., Ishikawa, T., Omata, M., Nagai, R., Kurihara, H., Asano, T., 2003. Structural and functional characterization of gastric mucosa and central nervous system in histamine H(2) receptor-null mice. Eur. J. Pharmacol. 468, 47–58.

Hollande, F., Choquet, A., Blanc, E.M., Lee, D.J., Bali, J.P., Baldwin, G.S., 2001. Involvement of phosphatidylinositol 3-kinase and mitogen-activated protein kinases in glycine-extended gastrin-induced dissociation and migration of gastric epithelial cells. J. Biol. Chem. 276, 40402–40410.

Karam, S.M., Leblond, C.P., 1992. Identifying and counting epithelial cell types in the "corpus" of the mouse stomach. Anat. Rec. 232, 231–246.

Karam, S.M., Leblond, C.P., 1993a. Dynamics of epithelial cells in the corpus of the mouse stomach. I. Identification of proliferative cell types and pinpointing of the stem cell. Anat. Rec. 236, 259–279.

Karam, S.M., Leblond, C.P., 1993b. Dynamics of epithelial cells in the corpus of the mouse stomach. II. Outward migration of pit cells. Anat. Rec. 236, 280–296.

Karam, S.M., Leblond, C.P., 1993c. Dynamics of epithelial cells in the corpus of the mouse stomach. III. Inward migration of neck cells followed by progressive transformation into zymogenic cells. Anat. Rec. 236, 297–313.

Karam, S.M., Leblond, C.P., 1993d. Dynamics of epithelial cells in the corpus of the mouse stomach. V. Behavior of entero-endocrine and caveolated cells: general conclusions on cell kinetics in the oxyntic epithelium. Anat. Rec. 236, 333–340.

Karam, S., Leblond, C.P., 1995. Origin and migratory pathways of the eleven epithelial cell types present in the body of the mouse stomach. Microsc. Res. Tech. 31, 193–214.

Kobayashi, T., Tonai, S., Ishihara, Y., Koga, R., Okabe, S., Watanabe, T., 2000. Abnormal functional and morphological regulation of the gastric mucosa in histamine H2 receptor-deficient mice. J. Clin. Invest. 105, 1741–1749.

Koh, T.H., J.R. Goldenring, J.R., Ito, S., Mashimo, H., Kopin, A.S., Varro, A., Dockray, G.J., Wang, T.C., 1997. Gastrin deficiency results in altered gastric differentiation and decreased colonic proliferation in mice. Gastroenterology 113, 1015–1025.

Langhans, N., Rindi, G., Chiu, M., Rehfeld, J.F., Ardman, B., Beinborn, M., Kopin, A.S., 1997. Abnormal gastric histology and decreased acid production in cholecystokinin-B/gastrin receptor-deficient mice. Gastroenterology 112, 280–286.

Li, Q., Karam, S.M., Gordon, J.I., 1996. Diphtheria toxin-mediated ablation of parietal cells in the stomach of transgenic mice. J. Biol. Chem. 271, 3671–3676.

Lloyd, K.C., Amirmoazzami, S., Friedik, F., Chew, P., Walsh, J.H., 1997. Somatostatin inhibits gastrin release and acid secretion by activating sst2 in dogs. Am. J. Physiol. 272, G1481–G1488.

Matsui, M., Motomura, D., Karasawa, H., Fujikawa, T., Jiang, J., Komiya, Y., Takahashi, S., Taketo, M.M., 2000. Multiple functional defects in peripheral autonomic organs in mice lacking muscarinic acetylcholine receptor gene for the M3 subtype. Proc. Natl. Acad. Sci. U. S. A. 97, 9579–9584.

Mutoh, H., Hakamata, Y., Sato, K., Eda, A., Yanaka, I., Honda, S., Osawa, H., Kaneko, Y., Sugano, K., 2002. Conversion of gastric mucosa to intestinal metaplasia in Cdx2-expressing transgenic mice. Biochem. Biophys. Res. Commun. 294, 470–479.

Nagata, A., Ito, M., Iwata, N., Kuno, J., Takano, H., Minowa, O., Chihara, K., Matsui, T., Noda, T., 1996. G protein-coupled cholecystokinin-B/gastrin receptors are responsible for physiological cell growth of the stomach mucosa in vivo. Proc. Natl. Acad. Sci. U. S. A. 93, 11825–11830.

Ogawa, T., Maeda, K., Tonai, S., Kobayashi, T., Watanabe, T., Okabe, S., 2003. Utilization of knockout mice to examine the potential role of gastric histamine H2-receptors in Menetrier's disease. J. Pharmacol. Sci. 91, 61–70.

Shindo, T., Manabe, I., Fukushima, Y., Tobe, K., Aizawa, K., Miyamoto, S., Kawai-Kowase, K., Moriyama, N., Imai, Y., Kawakami, H., Nishimatsu, H., Ishikawa, T., Suzuki, T., Morita, H., Maemura, K., Sata, M., Hirata, Y., Komukai, M., Kagechika, H., Kadowaki, T., Kurabayashi, M., Nagai, R., 2002. Kruppel-like zinc-finger transcription factor KLF5/BTEB2 is a target for angiotensin II signaling and an essential regulator of cardiovascular remodeling. Nat. Med. 8, 856–863.

Stepan, V.M., Krametter, D.F., Matsushima, M., Todisco, A., Delvalle, J., Dickinson, C.J., 1999. Glycine-extended gastrin regulates HEK cell growth. Am. J. Physiol. 277, R572–R581.

Tanaka, S., Hamada, K., Yamada, N., Sugita, Y., Tonai, S., Hunyady, B., Palkovits, M., Falus, A., Watanabe, T., Okabe, S., Ohtsu, H., Ichikawa, A., Nagy, A., 2002. Gastric acid secretion in L-histidine decarboxylase-deficient mice. Gastroenterology 122, 145–155.

Wolfsen, H.C., Carpenter, H.A., Talley, N.J., 1993. Menetrier's disease: a form of hypertrophic gastropathy or gastritis? Gastroenterology 104, 1310–1319.

Yamada, T., Alpers, D., Owyang, C., Powell, D., Silverstein, F., 1995. Textbook of gastroenterology, in Gastritis, duodenitis, and associated ulcerative lesions vol. 1.

J Hum Genet (2004) 49:629–634
DOI 10.1007/s10038-004-0199-3

ORIGINAL ARTICLE

Hajime Nawata · Senji Shirasawa · Naoki Nakashima
Eiichi Araki · Jun Hashiguchi · Seibei Miyake
Teruaki Yamauchi · Kazuyuki Hamaguchi
Hironobu Yoshimatsu · Haruo Takeda
Hideo Fukushima · Takayuki Sasahara
Kohei Yamaguchi · Noriyuki Sonoda · Tomoko Sonoda
Masahiro Matsumoto · Yoshiya Tanaka
Hidekatsu Sugimoto · Hirotaka Tsubouchi
Toyoshi Inoguchi · Toshihiko Yanase
Nakayasu Wake · Kenziro Narazaki · Takashi Eto
Fumio Umeda · Mitsuhiro Nakazaki · Junko Ono
Takashi Asano · Yasuko Ito · Shoichi Akazawa
Iwaho Hazegawa · Nobuyuki Takasu
Moritsugu Shinohara · Takeshi Nishikawa
Seiho Nagafuchi · Toshimitsu Okeda
Katsumi Eguchi · Masanori Iwase · Mayuko Ishikawa
Masayuki Aoki · Naoto Keicho · Norihiro Kato
Kazuki Yasuda · Ken Yamamoto · Takehiko Sasazuki

Genome-wide linkage analysis of type 2 diabetes mellitus reconfirms the susceptibility locus on 11p13–p12 in Japanese

Received: 9 July 2004 / Accepted: 9 August 2004 / Published online: 14 October 2004

Abstract Type 2 diabetes mellitus is a heterogeneous disorder, and the development of type 2 diabetes mellitus is associated with both insulin secretion defect and insulin resistance. The primary metabolic defect leading to type 2 diabetes mellitus has been thought to be varied among populations, especially in Japanese and Caucasians. Here, we have done the genome-wide scan for type 2 diabetes mellitus using 102 affected Japanese sib-pairs to identify the genetic factors predisposing to type 2 diabetes mellitus. Nonparametric linkage analysis showed one suggestive evidence for linkage to 11p13–p12 [*D11S905*: two-point maximum LOD score (MLS) of 2.89 and multipoint MLS of 2.32] and one nominally significant evidence for linkage to 6q15–q16 (*D6S462*: two-point MLS of 2.02). Interestingly, the 11p13–p12 region was reported to be a susceptibility locus for Japanese type 2 diabetes mellitus with suggestive evidence of linkage, and *D11S905* was within 5 cM to *D11S935* with the highest MLS in the previous linkage analysis reported. The only overlapped susceptibility region with suggestive evidence of linkage for Japanese type 2 diabetes mellitus was *D11S935–D11S905* among

H. Nawata · N. Sonoda · H. Tsubouchi · T. Inoguchi
T. Yanase · T. Eto
Department of Medicine and Bioregulatory Science,
Graduate School of Medical Sciences, Kyushu University,
Fukuoka, Japan

S. Shirasawa · M. Ishikawa
Department of Pathology, Research Institute,
International Medical Center, Tokyo, Japan

N. Nakashima
Department of Medical Informatics,
Kyushu University Hospital, Fukuoka, Japan

E. Araki · T. Nishikawa
Department of Metabolic Medicine,
Faculty of Medical and Pharmaceutical Sciences,
Kumamoto University, Kumamoto, Japan

J. Hashiguchi
Tenposan Clinic, Kagoshima, Japan

S. Miyake
Sasebo Central Hospital, Nagasaki, Japan

T. Yamauchi
Yukuhashi Central Hospital, Fukuoka, Japan

K. Hamaguchi · H. Yoshimatsu
Department of Internal Medicine 1,
Faculty of Medicine, Oita University, Oita, Japan

H. Takeda
Yatsushiro General Hospital, Kumamoto, Japan

H. Fukushima
Public Tamana Central Hospital, Kumamoto, Japan

T. Sasahara
Omuta Tenryo Hospital, Fukuoka, Japan

K. Yamaguchi
Oita Prefectural Hospital, Oita, Japan

T. Sonoda
Sonoda Clinic, Kagoshima, Japan

M. Matsumoto
Kitakyushu Municipal Medical Center, Fukuoka, Japan

Y. Tanaka
First Department of Internal Medicine, School of Medicine,
University of Occupational & Environmental Health,
Fukuoka, Japan

H. Sugimoto
Sugimoto Clinic, Fukuoka, Japan

N. Wake
National Health Insurance Takachiho Town Hospital,
Miyazaki, Japan

K. Narazaki
Narazaki Clinic, Fukuoka, Japan

F. Umeda
Diabetology and Endocrinology Division of Internal Medicine,
Fukuoka Medical Association Hospital, Fukuoka, Japan

M. Nakazaki
Department of Cardiovascular,
Respiratory & Metabolic Medicine
Graduate School of Medicine, Kagoshima University,
Kagoshima, Japan

J. Ono
Department of Laboratory Medicine,
School of Medicine,
Fukuoka University, Fukuoka, Japan

T. Asano
First Department of Internal Medicine,
School of Medicine,
Fukuoka University, Fukuoka, Japan

Y. Ito
Furugou Clinic, Oita, Japan

S. Akazawa
Shin-Koga Hospital, Fukuoka, Japan

I. Hazegawa
Kamiamakusa General Hospital, Kumamoto, Japan

N. Takasu
Department of Endocrinology and Metabolism,
Faculty of Medicine, University of the Ryukyus,
Okinawa, Japan

M. Shinohara
National Health Insurance Matsubase Town Hospital,
Kumamoto, Japan

S. Nagafuchi
Department of Medicine and Biosystemic Science,
Graduate School of Medical Sciences,
Kyushu University, Fukuoka, Japan

T. Okeda
Shin-Kokura Hospital, Fukuoka, Japan

K. Eguchi
First Department of Internal Medicine,
Graduate School of Biomedical Sciences,
Nagasaki University, Nagasaki, Japan

M. Iwase
Department of Medicine and Clinical Science,
Graduate School of Medical Sciences,
Kyushu University, Fukuoka, Japan

M. Aoki · K. Yamamoto
Medical Institute of Bioregulation, Kyushu University,
Fukuoka, Japan

N. Keicho · N. Kato · K. Yasuda
Research Institute,
International Medical Center of Japan,
Tokyo, Japan

T. Sasazuki (✉)
International Medical Center of Japan, 1-21-1 Toyama,
Shinjuku-ku, Tokyo 162-8655, Japan
E-mail: sasazuki@nciryo.hosp.go.jp
Tel.: +81-3-32027181
Fax: +81-3-52730113

the three reports including this study. These results taken together suggest that a susceptibility gene for type 2 diabetes mellitus in Japanese will reside in 11p13–p12.

Keywords Type 2 diabetes mellitus · Japanese · Affected sib-pairs · Linkage · Chromosome 11p

Introduction

Type 2 diabetes mellitus is one of the most common diseases, and its prevalence is dramatically increasing worldwide (Zimmet et al. 2001). Type 2 diabetes mellitus is a heterogeneous disorder, and the development of type 2 diabetes mellitus is associated with both insulin secretion defect and insulin resistance. Japanese patients with type 2 diabetes mellitus were reported to be characterized by a lower body mass index (BMI) and lower fasting insulin levels than other populations (Ehm et al. 2000). Insulin secretion defect is thought to be the primary defect in Japanese (Kadowaki et al. 1984) whereas impaired insulin sensitivity is the first metabolic defect predisposing to the development of type 2 diabetes mellitus in Caucasians (Martin et al. 1992). These findings suggest that Japanese individuals with type 2 diabetes mellitus will have a different genetic risk factor, which affects the responsiveness of insulin secretion to glucose, from other populations. Therefore, we need to identify the susceptibility genes for the development of type 2 diabetes mellitus in Japanese to start a primary prevention based on genetic information and to develop the personalized medicine for type 2 diabetes mellitus in Japanese. So far, two whole-genome linkage analyses were carried out using 224 affected sib-pairs (ASPs) from 159 Japanese families (Mori et al. 2002) and 256 ASPs from 164 Japanese families (Iwasaki et al. 2003), besides the analysis of 45 ASPs from 18 Japanese American families (Ehm et al. 2000). The Japanese people may have advantages in the genetic analysis of polygenic disorders like diabetes since they are supposed to be a relatively homogeneous population. However, the two previous reports on the ASP analysis in Japanese did not give good overlapping regions, except for 6p and 2q, and it has been argued that the replication by the third panel is indispensable for genetic susceptibility loci in Japanese. Here, we have carried out the third whole-genome linkage analysis on 102 ASPs from 102 Japanese families to identify the susceptibility loci for the development of type 2 diabetes mellitus.

Subjects and methods

One hundred and two ASPs with type 2 diabetes mellitus from 102 families were collected mainly from the Kyushu region in southwestern Japan. Parents and other siblings were not available in this study. The participants were interviewed and examined and gave written informed consent. This project was approved by the ethics committees of the related institutes. The diagnosis of type 2 diabetes mellitus was made based on the American Diabetes Association's 1997 criteria (Expert

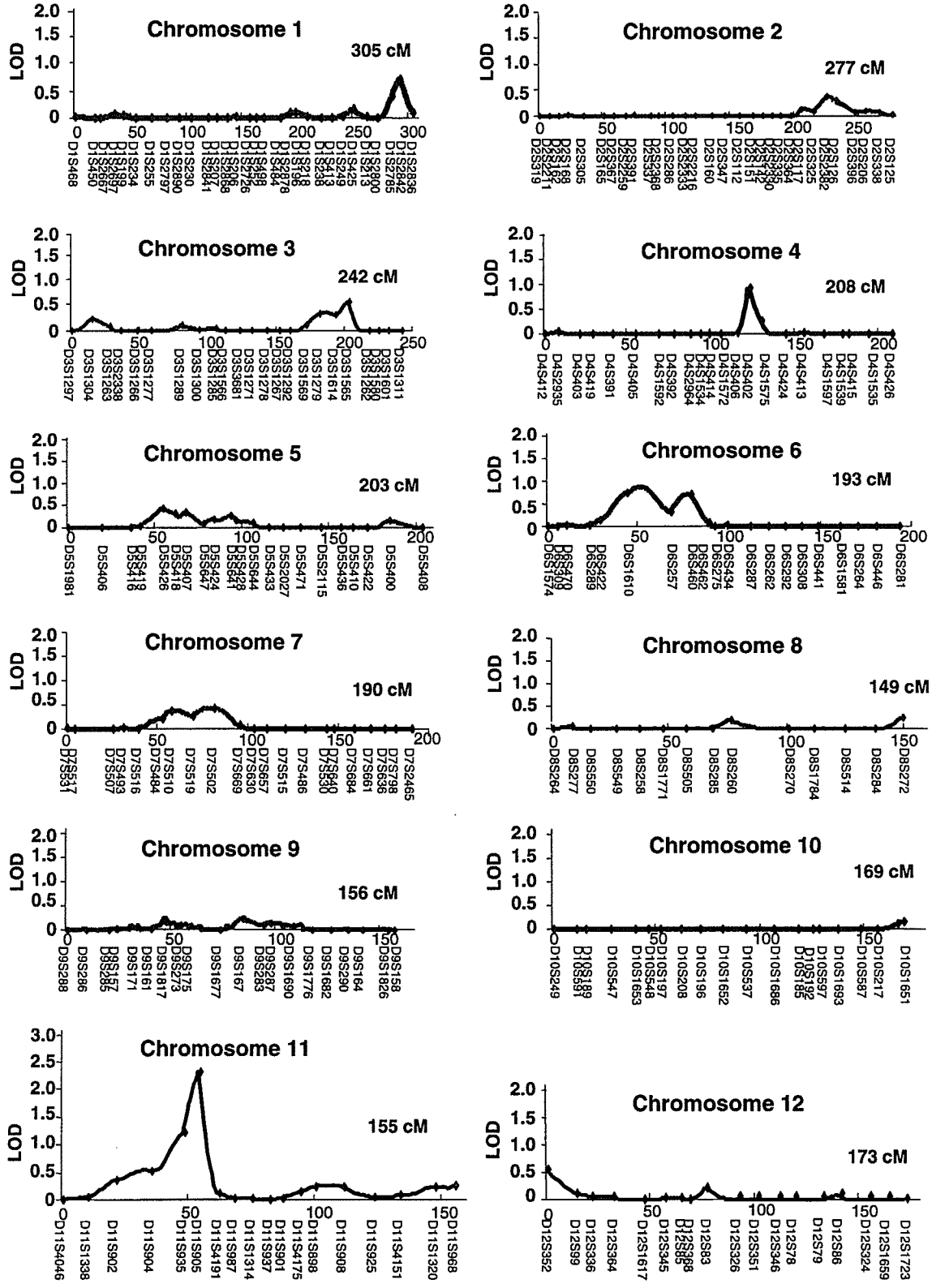

Fig. 1 Multipoint LOD score map of type 2 diabetes mellitus by linkage analysis of 382 markers in 102 affected sib-pairs. The *horizontal axis* is cM position from the p-terminal end of the chromosome

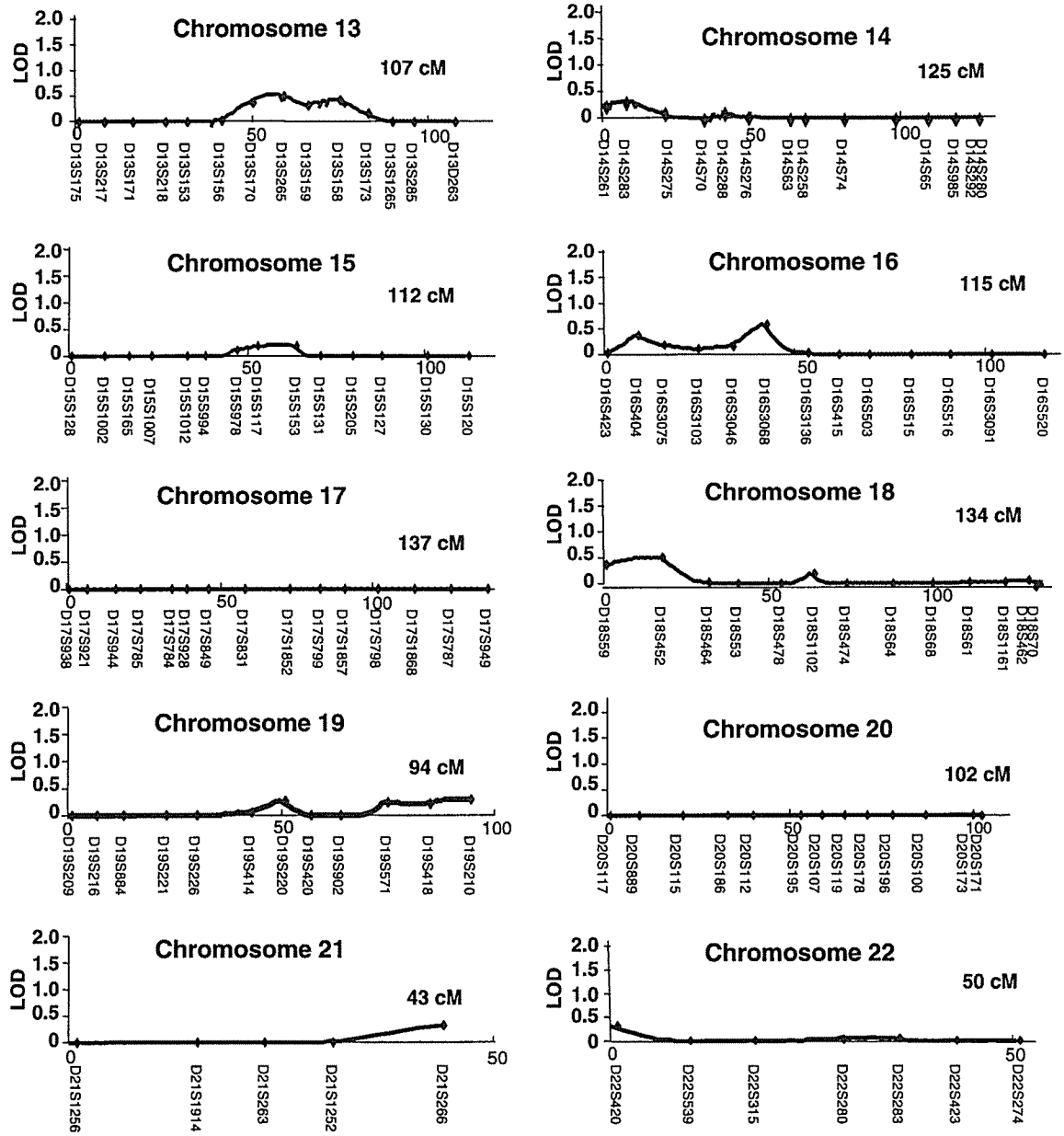

Fig. 1 (Continued)

Committee on the Diagnosis and Classification of Diabetes Mellitus 1997).

Genomic DNA was isolated from peripheral blood cells using QIAamp DNA Blood Midi Kits (Qiagen). Autosomal whole-genome screening of 382 microsatellite markers (ABI PRISM Linkage Mapping Set Version 2.5-MD10) was performed using an ABI 3730 automatic sequencer (Applied Biosytems). Analyses and assignment of the marker alleles were done with ABI PRISM GeneMapper Software Version 3.0, and 376 markers were available for the linkage analysis. Nonparametric two-point and multipoint linkage analyses were performed with the MAPMAKER/SIBS program (Kruglyak and Lander 1995), as described (Sakai et al. 2001). Heterozygosities of the markers were estimated

Table 1 Results of linkage analysis of type 2 diabetes mellitus and markers showing evidence of linkage

Marker	cM[a]	Analysis	MLS	*P*
D6S462	89	Two-point	2.02	0.0097
D11S905	54	Two-point	2.89	0.0013
		Multipoint	2.32	0.0048

[a]The distance of the marker form the p-terminal end of the chromosome in cM

with Merlin program (Abecasis et al. 2002) for all individuals.

Results and discussion

Whole autosomal genome linkage analysis using the ASP method with 382 microsatellite markers was carried out on 102 Japanese ASPs with type 2 diabetes mellitus. In this study, the average heterozygosity of the markers used was 0.72. Multipoint linkage analysis at all autosomal chromosomes using the MAPMAKER/SIBS program revealed only one region on chromosome 11p where the MLS was >1 (Fig. 1). The highest multipoint MLS was 2.32 ($P=0.0048$) at *D11S905* (Fig. 1, Table 1). On the other hand, two-point linkage analysis revealed two markers, *D11S905* (MLS = 2.89, $P=0.0013$) and *D6S462* (MLS = 2.02, $P=0.0097$), with evidence of linkage to type 2 diabetes mellitus (Table 1). Although the heterozygosity of *D11S905* was 0.30 in this study, it was 0.75 and 0.60 in our two reports using ASPs (Sakai et al. 2001; Aoki et al. 2004), indicating that *D11S905* itself will be useful in the genetic analysis in terms of heterozygosity in the Japanese population, and particular alleles of *D11S905* might be associated with type 2 diabetes mellitus. The 11p13–p12 region was reported to be linked to Japanese type 2 diabetes mellitus specifically, in which multipoint analysis showed the highest MLS of 3.08 near *D11S935* (Mori et al. 2002). The distance between *D11S905* and *D11S935* is about 5 cM. These findings together suggest that the 11p13–p12 region will be a susceptibility region for Japanese type 2 diabetes mellitus.

In addition to *D11S905*, one nominally significant evidence of linkage was detected at *D6S462* (MLS of 2.02) by two-point analysis. However, the multipoint MLS at *D6S462* was 0.08, and two other reports did not show evidence of linkage to this region (Mori et al. 2002; Iwasaki et al. 2003), suggesting that 6q15–q16 might not be a susceptibility region for type 2 diabetes mellitus. Two susceptibility regions for type 2 diabetes mellitus in Japanese, chromosome 2 (236.8 cM) and chromosome 6 (42.2 cM), were reported to be overlapped between the two previous linkage studies (Iwasaki et al. 2003). However, the MLS at these two loci were <1 (Iwasaki et al. 2003). Among the three reports including this study, the overlapped susceptibility region with suggestive evidence of linkage for Japanese type 2 diabetes mellitus was *D11S935–D11S905* only.

In conclusion, we have reconfirmed that the evidence of linkage for type 2 diabetes mellitus in Japanese to 11p13–p12 and 11p13–p12 will be a promising region for future studies on identification of susceptibility genes for type 2 diabetes mellitus in Japanese.

Acknowledgements We thank all patients for participating in this study, T. Amano in Kyushu University and T. Baba in SRL, Inc., for collecting the samples, and A. Murakami, E. Yachi, K. Ohki, and T. Fujimoto for technical assistance. This work was supported by the Program for Promotion of Fundamental Studies in Health Sciences of Pharmaceuticals and Medical Devices Agency (PMDA).

Appendix

Collaborating groups listed in alphabetic order: Nobuyuki Abe (Abe Diabetes Clinic), Katsumi Eguchi (Nagasaki University), Nobuaki Fujio (Beppu Medical Center), Masafumi Haji (Kyushu Rosai Hospital), Mine Harada (Kyushu University), Sinsuke Hiramatsu (Kyushu Medical Center), Mitsuo Iida (Kyushu University), Minako Imamura (Kyushu University), Hidehiro Ishii (Kitakyushu Municipal Medical Center), Eiji Kawasaki (Nagasaki University), Kunihisa Kobayashi (Kyushu University), Ichiro Komiya (University of the Ryukyus), Shiori Kondo (Matsuyama Red Cross Hospital), Yasuko Kono (Imamura Hospital), Nobuyuki Koriyama (Kagoshima University), Minoru Kuriyama (Social Health Insurance Inatsuki Hospital), Kazunari Matsumoto (Sasebo Central Hospital), Kazuo Mimura (Fukuoka Medical Association Hospital), Isao Morimoto (Inoue Hospital), Mieko Nakayama (Kyushu University), Shyoichi Natori (Aso Iizuka Hospital), Yosuke Okada (University of Occupational & Environmental Health), Haruka Sasaki (Fukuoka University), Naotaka Sekiguchi (Kyushu University), Yasunori Sera (Sasebo Central Hospital), Michio Shimabukuro (University of the Ryukyus), Yuji Tajiri (Fukuoka Medical Association Hospital), Chuwa Tei (Kagoshima University), Maiko Tsuda (Kitakyushu Municipal Medical Center), Takero Uemura (Yatsushiro General Hospital), Eiji Kawasaki (Nagasaki University).

References

Abecasis GR, Cherny SS, Cookson WO, Cardon LR (2002) Merlin-rapid analysis of dense genetic maps using sparse gene flow trees. Nat Genet 30:97–101

Aoki M, Yamamura Y, Noshiro H, Sakai K, Yokota J, Kohno T, Tokino T, Ishida S, Ohyama S, Ninomiya I, Uesaka K, Kitajima M, Shimada S, Matsuno S, Yano M, Hiratsuka M, Sugimura H, Itoh F, Minamoto T, Maehara Y, Takenoshita S, Aikou T, Katai H, Yoshimura K, Takahashi T, Akagi K, Sairenji M, Yamamoto K, Sasazuki T (2004) A full genome scan for gastric cancer. J Med Genet (in press)

Ehm MG, Karnoub MC, Sakul H, Gottschalk K, Holt DC, Weber JL, Vaske D, Briley L, Kopf J, McMillen P, Nguyen Q, Reisman M, Lai EH, Joslyn G, Shepherd NS, Bell C, Wagner MJ, Burns DK, ADA GENNID Study Group (2000) Genomewide search for type 2 diabetes mellitus susceptibility genes in four American populations. Am J Hum Genet 66:1871–1881

Expert Committee on the Diagnosis and Classification of Diabetes Mellitus (1997) Report of the expert committee on the diagnosis and classification of diabetes mellitus. Diabetes Care 20:1183–1197

Iwasaki N, Cox NJ, Wang Y-Q, Schwaz PEH, Bell GI, Honda M, Imura M, Ogata M, Saito M, Kamatani N, Iwamoto Y (2003) Mapping genes influencing type 2 diabetes mellitus risk and BMI in Japanese subjects. Diabetes 52:209–213

Kadowaki T, Miyake Y, Hagura R, Akanuma Y, Kajinuma H, Kuzuya N, Takaku F, Kosaka K (1984) Risk factors for worsening to diabetes in subjects with impaired glucose tolerance. Diabetologia 26:44–49

Kruglyak L, Lander ES (1995) Complete multipoint sib-pair analysis of qualitative and quantitative traits. Am J Hum Genet 57:439–454

Martin BC, Warram JH, Krolewski AS, Bergman RN, Soeldner JS, Kahan CR (1992) Lancet 340:925–929

Mori Y, Otabe S, Dina C, Yasuda K, Populaire C, Lecoeur C, Vatin V, Durand E, Hara K, Okada T, Tobe K, Boutin P, Kadowaki T, Froguel P (2002) Genome-wide search for type 2 diabetes mellitus in Japanese affected sib-pairs confirms susceptibility genes on 3q, 15q, and 20q and identifies two new candidate loci on 7p and 11p. Diabetes 51:1247–1255

Sakai K, Shirasawa S, Ishikawa N, Ito K, Tamai H, Kuma K, Akamizu T, Tanimura M, Furugaki K, Yamamoto K, Sasazuki T (2001) Identification of susceptibility loci for autoimmune thyroid disease to 5q31–q33 and Hashimoto's thyroiditis to 8q23–q24 by multipoint affected sib-pair linkage analysis in Japanese. Hum Mol Genet 10:1379–1386

Zimmet P, Alberti KGMM, Shaw J (2001) Global and societal implications of the diabetes epidemic. Nature 414:782–787

Available online at www.sciencedirect.com
SCIENCE DIRECT
Molecular Brain Research 131 (2004) 119–125
MOLECULAR BRAIN RESEARCH
www.elsevier.com/locate/molbrainres

Research report

Differential regulation of the regulatory subunits for phosphatidylinositol 3-kinase in response to motor nerve injury

Takashi Okamoto[a,b], Kazuhiko Namikawa[a], Tomoichiro Asano[c], Kunio Takaoka[b], Hiroshi Kiyama[a,*]

[a]*Department of Anatomy and Neurobiology, Graduate School of Medicine, Osaka City University, 1-4-3 Asahimachi, Abenoku, Osaka 545-8585, Japan*
[b]*Department of Orthopaedic Surgery, Graduate School of Medicine, Osaka City University, Osaka 545-8585, Japan*
[c]*Department of Internal Medicine, Graduate School of Medicine, University of Tokyo, Tokyo 113-0033, Japan*

Accepted 28 August 2004
Available online 25 September 2004

Abstract

Type Ia phosphatidylinositol 3-kinase (PI3K) generates lipid products that operate as one of major second messengers following activation of tyrosine kinase receptors. PI3K is a heterodimer composed of a 110-kDa catalytic subunit and a regulatory subunit. In this study, we determined the expression of mRNA for the regulatory subunits after injury of rat hypoglossal nerves. In situ hybridization histochemistry revealed that the expression of PI3K regulatory subunit α isoforms (p85α, p55α, and p50α) was significantly enhanced in injured motor neurons, whereas other regulatory subunits such as p85β or p55γ were not detected. Of the α isoforms, the greatest increase was observed in p55α mRNA levels, while there were smaller increases in p85α and p50α mRNA expression. These results were confirmed by RT-PCR analysis. Further immunohistochemical analysis also confirmed the increased level of p55α protein in injured motor neurons. Taken together with the previously reported induction of the p110α catalytic subunit in injured neurons, these results suggest that PI3K, consisting of p55α and p110α, plays a crucial role in the process of nerve regeneration.

Theme: Development and regeneration
Topic: Regeneration

Keywords: Nerve injury; Hypoglossal nerve; PI3K; Phosphoinositide; Regulatory subunit; Rat

1. Introduction

Previous work has shown that a peripheral nerve injury induces an organized expression of a wide range of molecules belonging to intracellular signaling pathways. For instance, Akt/Protein kinase B (PKB), Shc, 14-3-3, extracellular signaling kinase 1 (ERK1), ERK kinase 1 (MEK1), and JAK2/3 were all up-regulated in regenerating motor neurons [21,28–30,35,43]. Of these molecules, we have shown the functional consequences of Akt-mediated signaling pathways during the regeneration of injured motor neurons [28]. Adenoviral gene transfer of constitutively activated Akt could rescue injured motor neurons in vivo. In addition, Akt promotes axonal elongation of injured adult rat hypoglossal nerves [28]. It was therefore concluded that Akt is one of the key signaling molecules during nerve regeneration. The well-established signaling molecule of Akt activation is phosphatidylinositol 3-kinase (PI3K) [3,4]. In response to growth factor stimulation, PI3K can phosphorylate phosphoinositides at the D-3 position of the inositol ring [42]. This lipid by-product of PI3K recruits the PH domain of Akt to the cell membrane, enables Akt kinase PDK1 to phosphorylate Akt, and thereby activates Akt [4]. In addition to the survival activity of PI3K via Akt, PI3K is involved in various cellular responses, including protein synthesis, glucose uptake, proliferation, membrane ruffling, receptor internalization,

* Corresponding author. Tel.: +81 666 45 3700; fax: +81 666 45 3702.
E-mail address: kiyama@med.osaka-cu.ac.jp (H. Kiyama).

0169-328X/$ - see front matter © 2004 Elsevier B.V. All rights reserved.
doi:10.1016/j.molbrainres.2004.08.015

and chemotaxis [4], indicating that some might play an important role during nerve regeneration.

On the basis of substrate specificity, PI3K can be categorized into three classes (I, II, and III). Among those subclasses, Class I PI3K plays a major role in generating the lipid product $PI(3,4,5)P_3$ following activation of receptor tyrosine kinases [34]. Class I PI3K is a heterodimer composed of a 110-kDa catalytic subunit and a regulatory subunit. The primary role of the regulatory subunit of PI3K is to recognize an upstream signal such as tyrosine kinase receptor and Gab-1 [13]. To date, five mammalian PI3K regulatory subunit isoforms have been identified, including two full-length versions of 85-kDa proteins (p85α and p85β), two 55-kDa proteins (p55α and p55γ), and one 50-kDa protein p50α [39]. The alpha isoforms, p85α, p55α, and p50α, are splice variants derived from a single gene, while the isoforms p85β and p55γ originate from different genes [8]. However, the biological significance of this diversity is poorly understood even though all five isoforms are abundantly expressed in neurons of the rat brain [16,33]. Although the expression of mRNA for the PI3K catalytic subunit p110α is enhanced in injured motor neurons [19], the expression of any PI3K regulatory subunits following nerve injury has yet to be determined. In this study, we have focused on the members belonging to Class I because Class I PI3K is the primary group for the production of $PI(3,4,5)P_3$, which is important for the various intracellular signaling in vivo. We demonstrated that the expression of Class I PI3K regulatory subunits is differentially regulated in injured motor neurons, suggesting there are functional differences between the regulatory subunits during nerve regeneration.

2. Materials and methods

2.1. Animals and surgery

Adult male Wistar rats weighing 150–200 g (6–8 weeks old, total number of animal: 55) were anesthetized with pentobarbital (45 mg/kg). They were placed in a supine position and their right hypoglossal nerves were carefully exposed. The nerve was then cut was with a pair of scissors just proximal to its bifurcation at the hyoid bone.

2.2. In situ hybridization

The techniques used were essentially as described previously [29]. Animals (three rats at each time point) were decapitated 1, 3, 5, 7, 14, 28, and 49 days after surgery under deeply anesthesia (diethyl ether). Their brains were quickly removed and frozen on powdered dry ice. The 16-μm-thick sections were cut on a cryostat, thaw-mounted onto 3-aminopropyltriethoxysilane coated slides, and stored at −80 °C for later use. The following cDNA fragments were used as probes: common (1582-2170 of the accession number D64045); p85α (1-311 of the accession number D64045); p55α (-146-96 of the accession number D64048); p50α (-167-18 of the accession number D78486); p85β (-36-310 of the accession number D64046); and p55γ (97-547 of the accession number D64047) [33]. The antisense RNA probe for the common recognizes common regions of p85α, p55α, and p50α. The antisense RNA probes for p85α, p55α, p50α, p85β, and p55γ recognize their specific regions. The sections were fixed in 4% paraformaldehyde in 0.1 M phosphate buffer (PB) for 20 min, washed in PB, treated with 10 μg/ml proteinase K in 50 mM Tris–HCl and 5 mM EDTA for 10 min, and then returned to the fixative solution. After washing in distilled water, the sections were acetylated with 0.25% acetic anhydride in 0.1 M triethanolamine, rinsed with PB, dehydrated in an ascending ethanol series (70%, 95% and 100%), defatted in chloroform, rinsed in ethanol, and then air dried. The [α-^{35}S] UTP-labeled antisense RNA probes were prepared by in vitro transcription of each cDNA using T3 or T7 RNA polymerase (Promega, Madison, WI, USA) and [α-^{35}S] UTP. The labeled probes (5×10^5 cpm/μl) in hybridization buffer (50% deionized formamide, 0.3 M NaCl, 20 mM Tris–HCl, 5 mM EDTA, 10 mM PB, 10% dextran sulfate, 1×Denhardt's solution, 0.2% sarcosyl, 500 μg/μl yeast transfer RNA, and 200 μg/ml salmon sperm DNA) were denatured for two min in boiling water, quenched on ice, and placed on the sections. Hybridization was performed overnight in a humid chamber at 55 °C. Hybridized sections were briefly rinsed five times in saline sodium citrate buffer (SSC) and 1% 2-mercaptoethanol at 55 °C, and then washed in 50% deionized formamide, 2×SSC, and 10% 2-mercaptoethanol (high stringency buffer) for 30 min at 65 °C. After rinsing the sections in RNase buffer (0.5 M NaCl, 10 mM Tris–HCl, and 1 mM EDTA), they were treated with 1 μg/ml RNase-A in RNase buffer for 30 min at 37 °C and washed again in RNase buffer. Sections were then incubated in high stringency buffer again as described above, rinsed with 2×SSC and 0.1×SSC for 10 min each at room temperature, dehydrated in an ascending ethanol series, and then air dried. Sections were then exposed to X-ray film for 2 weeks and then dipped in Kodak NTB2 emulsion diluted 6:4 in water. Sections were then exposed for 5–6 weeks at 4 °C, developed in Kodak D-19 developer, counterstained with thionine, dehydrated in a graded series of ethanol to xylene, and coverslips mounted before examination by a microscope.

2.3. Relative quantification of mRNA

The relative optical density of signals on the X-ray film was measured using an Image Analysis System (NIH Image, National Institute of Health, USA). The defined area occupied by autoradiographic grains in the hypoglossal nuclei was measured bilaterally on the X-ray film using an image analyzer. The measured background value for cerebellar white matter was subtracted from the value for

hypoglossal nuclei, and the difference defined 'the optical density unit.' The optical density units from the right (injured) and the left (control) hypoglossal nuclei on the identical section were determined. For statistical analysis, at least four sections from three rats per time point were studied. Statistically significant difference was assessed by paired *t*-test.

2.4. RT-PCR analysis

Operations were performed on adult male Wistar rats weighing 150–200g (6–8 weeks old) and killed on postoperative day 7 under deeply anesthesia. Reverse transcription–polymerase chain reaction (RT-PCR) was conducted as described by Honma et al. [12] with a slight modification. The total RNA derived from hypoglossal nuclei on either side was isolated and purified using the acid guanidine isothiocyanate/phenol/chloroform extraction (AGPC) method [5]. Aliquots from the RT reaction were used for PCR amplification using primer pairs for the ubiquitously expressed glyceraldehydes-3-phosphate dehydrogenase (GAPDH) as an internal control. Activating transcription factor-3 (ATF-3), which is induced after a hypoglossal axotomy, was used as a positive control. The amplifying cycle counts were 34 for the detection of PI3K regulatory subunits except p55γ, 32 for the detection of p55γ and ATF-3, and 20 for the detection of GAPDH.

Specific primers for the detection of mRNA for each PI3K regulatory subunit were used for RT-PCR. The primers used were as follows: for p85α, 668–688 and 1218–1237 of D64045; for p55α, 15–34 and 408–427 of D64048; for p50α, 1–20 and 318–337 of D78486; for p85β, 383–402 and 1034–1053 of D64046; for p55γ, 7–28 and 423–442 of D64047; for GAPDH, 836–855 and 1149–1168 of NM017008; and for ATF–3, 165–187 and 688–708 of M63282. The reaction products were separated electrophoretically on a 1% agarose gel and visualized by staining with ethidium bromide.

2.5. Immunohistochemistry

Animals were perfused at postoperative day 7. The brains were quickly removed and fixed in a 4% paraformaldehyde solution. Brains were postfixed in the same fixative for 3 days, and then immersed in phosphate-buffered saline (PBS) containing 25% sucrose before being sectioned. The 20-μm-thick sections were cut on a cryostat and floated in 6-well cell culture dishes containing PBS. The primary antibody against the N-terminal SH2 region of rat p85α, which recognizes all three α-isoforms of the PI3K regulatory subunit, was purchased from UBI (Lake Placid, NY, USA) [38]. A p55α-specific antibody was raised and characterized as previously described [15,16,33]. The primary antibodies were used at a dilution of 1:500. The sections were covered with 5% normal goat serum in PBS for 30 min and incubated with the primary antibodies over two nights. After being washed in PBS, the sections were subsequently incubated with biotinylated goat anti-rabbit IgG antibody (Vector Laboratories, USA) at a dilution of 1:200 for 2 h, washed with PBS, and treated with an avidin–biotin complex mixture (Vector Laboratories). The sections were washed with PBS and finally reacted with 3,3-diaminobenzidine tetrahydrochloride and hydrogen peroxide to reveal a brown reaction product. For a histochemical specificity, we have also examined those processes without the primary antibody, and in this control the staining was negative.

3. Results

We performed in situ hybridization to evaluate the changes in expression of mRNA for the regulatory subunit

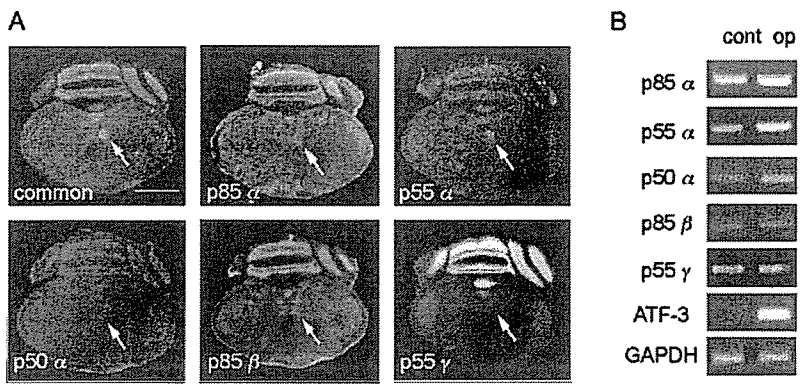

Fig. 1. Expression of mRNA for the PI3K regulatory subunit family members (p85α, p55α, p50α, p85β, and p55γ) after nerve injury. Film autoradiography of hybridized tissue sections for PI3K regulatory subunit family members 7 days after hypoglossal nerve transection (A). Only the common p85α, p55α, and p50α probes exhibited increased levels of mRNA on the operated side (right; arrows). The common sequence was a region common to all three α-isoforms. Scale bar=3 mm. Expression of mRNA for the PI3K regulatory subunit family members (p85α, p55α, p50α, p85β, and p55γ) in nerve injured hypoglossal nucleus determined by RT-PCR (B). In hypoglossal nuclei, p85α, p55α, and p50α mRNA level was higher on the injured sides compared with the uninjured side. However, the expression of p55γ and p85β on the injured side was weaker in hypoglossal nuclei. The expression of GAPDH mRNA was used as an internal control. ATF-3 mRNA expression was used as a positive control.

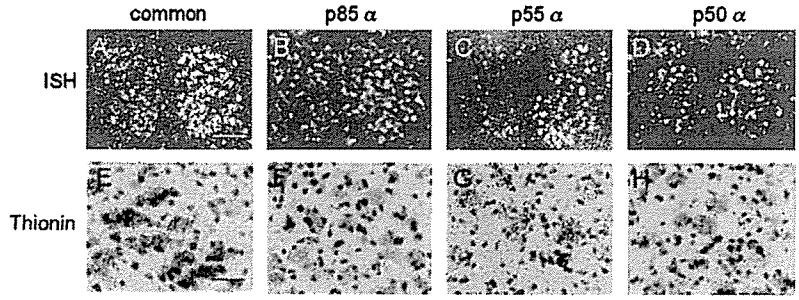

Fig. 2. Expression of mRNA for common (A and E), p85α (B and F), p55α (C and G), and p50α (D and H) in the hypoglossal nucleus 7 days after a hypoglossal nerve transection (right). Emulsion autoradiography of hybridized tissue sections for the PI3K regulatory subunit family members (common, p85α, p55α, and p50α) (A–D). Scale bars=0.2 mm. High-power bright field photographs counterstained with thionine showed that the hybridization signal (accumulation of silver grains) was found on injured motor neurons, but not on glial cells (E–H). Scale bars=50 μm.

of PI3K during nerve regeneration. A marked increase in the mRNA for the common region of the α-isoforms was observed in the autoradiographic film (Fig. 1A). As the sequence is common to all three α-isoforms, we next determined the expression of each isoform using isoform-specific RNA probes. mRNA for the three α-isoforms (p85α, p55α, and p50α) was up-regulated after nerve injury, whereas the levels of mRNA for the β-and γ-isoforms (p85β and p55γ) did not exhibit any changes. The most marked increases were observed in p55α mRNA expression (Fig. 1A), while p85α and p50α mRNA levels showed smaller increases (Fig. 1A). To confirm these increases, we measured the changes in mRNA for the PI3K regulatory subunit by RT-PCR (Fig. 1B). The increase in ATF-3 mRNA was measured as a positive control. The results obtained confirmed those attained by in situ hybridization. The expression of α-isoform mRNA was up-regulated in injured hypoglossal nucleus, whereas β and γ-isoform mRNA levels were not altered. The increase in p55α mRNA expression was the most marked (Fig. 1B).

Emulsion autoradiography was also used to determine the cell types expressing elevated levels of mRNA for all three α-isoforms (Fig. 2A–D). Counterstaining with thionine revealed an accumulation of hybridization signal in the large cells of the hypoglossal nucleus, suggesting that the mRNA for the three α-isoforms increased in injured hypoglossal motor neurons but not in the surrounding glial cells (Fig. 2E–H).

A semiquantitative analysis of the film autoradiogram showed that there were significant increases in the levels of mRNA for p85α, p55α, and p50α 1–14 days after nerve injury (Fig. 3). One day after nerve transection, there were slight increases in the levels of p50α mRNA in the ipsilateral hypoglossal nucleus and marked increases to a peak level after 5 days. The hybridization signal then gradually returned to control levels over the following 3 weeks. The hybridization signal for p55α mRNA in the ipsilateral hypoglossal nucleus increased after 1 day of nerve resection and increased markedly to a peak level after 7 days. The hybridization signal then gradually returned to control levels over the following 3 weeks. Of the three α-isoforms, p55α mRNA exhibited the greatest increases. The increase in p85α mRNA appeared relatively late and peaked 7 days after nerve injury. There was a tendency that those mRNA levels were slightly increased in the contralateral hypoglossal nuclei.

To determine the changes in subunit protein expression, we used two antibodies that can detect either common α-

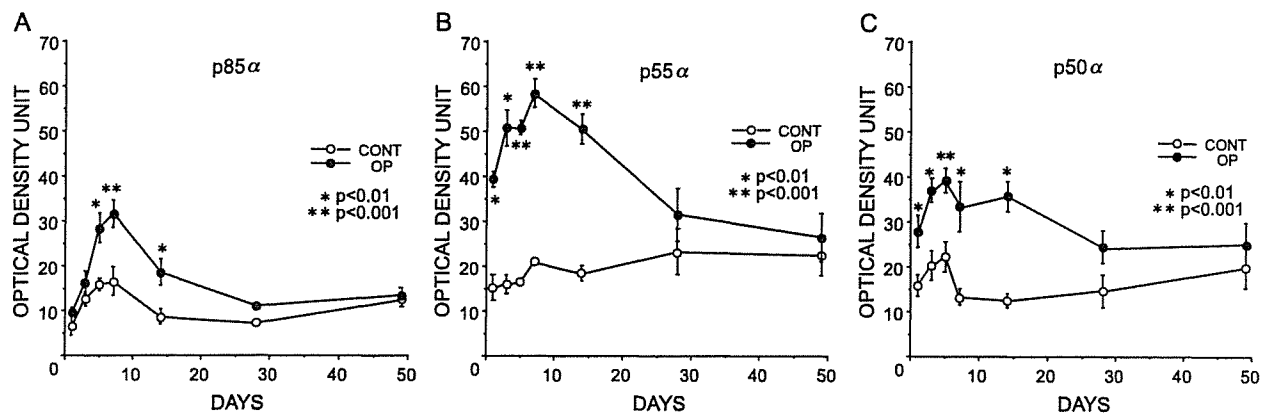

Fig. 3. Semiquantification of mRNA levels for the PI3K regulatory subunit α isoforms (p85α, p55α, and p50α) in both operated side (solid circle) and the contralateral control side (open circle). Each point shows the average intensity of positive signals and its S.E. as determined from the X-ray film autoradiograms. Statistically significant differences were determined by paired *t*-tests; *$p<0.01$ and **$p<0.001$).

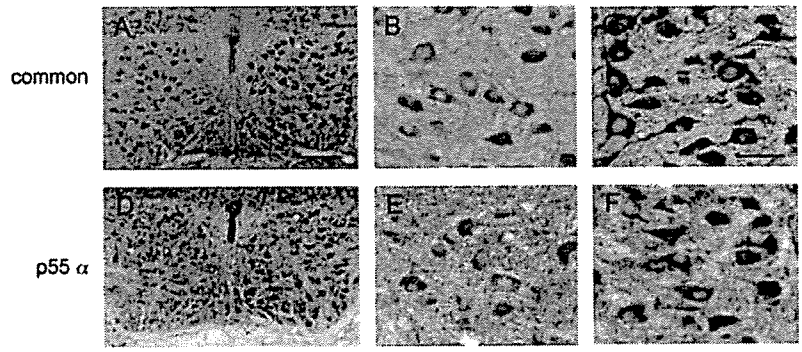

Fig. 4. Immunohistochemical detection of the α isoforms of the regulatory subunit for PI3K (common) and p55α in rat hypoglossal nuclei 7 days after nerve injury (operated side is on the right). Enhanced expression of the three α isoforms (common) and p55α were observed in injured hypoglossal nucleus (A and D). A high-power magnification also showed the three α isoforms (common) and p55α immunoreactivity in injured hypoglossal nucleus (C and F), whereas the intensity of staining in noninjured hypoglossal nucleus was weak (B and E). Scale bar=0.2 mm (A and D), and 50 μm (B, C, E and F).

subunits or specifically detect p55α subunits on the tissue sections. The specificity of these antibodies has been described previously [33,38]. Although the antibody, which detects the common N-terminal SH2 region of p85α revealed cytoplasmic staining of hypoglossal motor neurons in the noninjured nucleus, the staining was substantially greater in injured hypoglossal nucleus (Fig. 4A and C). Similarly, immunohistochemistry using the specific anti-p55α antibody revealed increased levels of p55α protein in the cytoplasm of injured hypoglossal neurons (Fig. 4D and F). These results clearly demonstrate that both the mRNA and protein of p55α were up-regulated in injured hypoglossal neurons but not in glial cells.

4. Discussion

In the present study, we determined whether the expression of PI3K regulatory subunits increased following motor nerve injury. Of the five isoforms examined, the mRNAs for the α isoforms of PI3K regulatory subunits (p85α, p55α, and p50α) are up-regulated in injured motor neurons. These isoforms have been shown to bind to p110α catalytic subunits via the p110 binding domains common to all three isoforms and thereby enhance p110α kinase activity. Since a previous report has shown that p110α expression is induced in injured motor neurons [19], a PI3K heterodimer composed of a p110α catalytic subunit and α isoforms of a regulatory subunit may play a key role in motor neuron regeneration. However, the expression profiles of all five regulatory subunits varied during nerve regeneration. The basal level of p85α mRNA is relatively high even in uninjured hypoglossal motor neurons and the up-regulation is relatively small. Similarly, moderate p110α mRNA hybridization signals were seen in the uninjured side (data not shown). These results suggest that p85α coupled with p110α are crucial in processes such as the maintenance of neuronal metabolism in normal neurons, as well as its role in neuronal regeneration. In contrast, almost no p55α and p50α expression was observed in noninjured motor neurons, but there is a substantial up-regulation of p55α mRNA and protein in response to nerve injury. Of all the PI3K regulatory subunits, p55α may be the most important in neuronal regeneration, although we need knockout or knock down strategy to conclude this. In terms of those mRNAs induction periods, Ito et al. [19] mentioned that the increased expression of p110α mRNA was seen during 2 weeks after nerve crush, but in our model the alteration of p110 mRNA was observed during 28 days after nerve cut (data not shown). This discrepancy would be due to the methods used (cut versus crush). Therefore, it seems that the mRNA alterations seen in p110 and p55α are in parallel. Our previous morphological study [26] demonstrated that outgrowth of thin regenerating axons into the frontal area of the tongue was firstly observed at 14 postoperative days, and presynaptic formation of neuromuscular junction (NMJ) was observed from 21 postoperative days. Under electron microscopic observation, reconstruction of new NMJs was observed within the interval between 21 and 28 days. These observations suggest that the alteration periods of p110 and p55α mRNAs are well corresponding to that of NMJ recovery. This may also support the involvement of PI3K in nerve regeneration.

There was a tendency that some mRNAs were slightly increased in the contralateral hypoglossal nuclei. Following peripheral nerve lesions, there are well-documented events that affect the contralateral nonlesioned structures. It is unclear whether these serve a biological purpose, but the existence of these effects implies the presence of unrecognized signaling mechanisms such as growth factors form the target organ, in this case from tongue [23].

PI3K has been shown to be involved in various cellular phenomena. In neuronal cells especially, previous studies have implicated PI3K activation in the regulation of neurite elongation [20], neuronal migration [2], synaptic plasticity [27], receptor internalization [44,45], and retrograde transport [24], in addition to mediating survival [28]. Although PI3K/Akt-induced survival activity might be one of its key biological functions in injured motor neurons [28], more recent papers have focused on its role in the regulation of cell

morphology or motility via cytoskeletal reorganization [6,7]. Such papers have shown that local activation of PI3K is crucial for the induction of correct cytoskeletal changes. In *Dictyostelium* cells or neutrophils, PI3K generates $PI(3,4)P_2$ and/or $PI(3,4,5)P_3$ at the leading edge of migrating cells in response to a gradient of chemoattractants, and PI3K localization to such a restricted region of the cells might be required for chemotaxis [9,14,40,41]. Similarly, the localization and activation of PI3K at the tip of the growth cones is necessary for determining the neuronal polarity during the specification and elongation of hippocampal axons [32]. Although the reason why such local activation of PI3K occurs remains unclear, p110 binding protein might be involved in determining the localization of p110 following factor stimulation. Here we found that of the PI3K regulatory subunits, p55α expression was the most prominent in response to nerve injury. Interestingly, p55α and p55γ contain a unique 34-amino-acid sequence in their N-terminus, which is not found in p85α or p50α. A previous biochemical study has shown that p55α exhibits strong and specific binding activity with tubulin via its unique sequence, although it is unknown whether this binding is direct [17]. Of the regulatory isoform overexpressing cells, insulin stimulated α/β tubulin-associated PI3K activity only in p55α overexpressing cells. In addition, p55α, but not p85α or p50α, was present in a purified microtubule assembly from rat brain [17]. Hence, injury-induced p55α in regenerating motor neurons might be a candidate molecule for the recruitment of PI3K to the correct site on the neuron, maybe to the microtubules. It is well known that reorganization of the cytoskeleton, including both actin filaments and microtubules, might be required for growing axon tips [25]. The regulation of actin dynamics may be a target for PI3K in regenerating axons, as PI3K activation could be involved in the regulation of actin filament polymerization by activating the Rho GTPase family [10]. However, PI3K might also have an affect on process formation or the maintenance of neurites via control of the microtubule network [22,31]. Thus, the induction of p55α in injured motor neurons (the present study) and its binding activity with tubulin [17] suggests that PI3K activity may be involved in the modification of the microtubule itself or its related molecules rather than actin dynamics during motor nerve regeneration.

Another specific function of p55α is also likely. Recent papers have shown that each isoform has a specific role in signal transduction activated by individual receptor tyrosine kinases [18,37]. For example, Inukai showed that each regulatory subunit exhibited a different response in both its association with the receptor tyrosine kinase complex, and signal transduction to their effectors [18]. These phenomena remind us that p55α is a more effective signal transducer than other isoforms, at least, in injured motor neurons. For motor neurons, GDNF would be the most effective survival promoting factor, and its signal transducing receptor, RET, was markedly up-regulated in injured motor neurons [36]. Of the α isoforms, at least p85α can bind GDNF-stimulated RET receptor complexes via a Gab-1/2 adaptor protein, and thereby transmit the evoked signal to the p110-Akt cascade [1,11]. However, whether other isoforms are more efficient than p85α in response to GDNF is still unclear. Such an isoform-specific response to GDNF and other neurotrophic factors should be investigated in further studies.

In summary, we have shown that there are increased levels of the PI3K regulatory subunit p55α in motor neurons following a nerve injury, although its precise role in signal transduction within injured neurons remains unclear. Further study is needed to elucidate its biological role in regenerating neurons.

Acknowledgement

We are grateful to Dr. Y. Yamano (Seikeikai Hospital, Osaka, Japan) and Prof. H. Mori (Osaka City University) for their encouragement. We are also grateful to C. Kadono and T. Ogawa for technical assistance, and E. Fukui for secretarial assistance. This study was supported in part by grants from the Ministry of Health, Labor and Welfare of Japan, the Ministry of Education, Science, Technology, Sports and Culture, the Novartis Foundation, and the Osaka Gas Foundation.

References

[1] V. Besset, R.P. Scott, C.F. Ibanez, Signaling complexes and protein–protein interactions involved in the activation of the Ras and phosphatidylinositol 3-kinase pathways by the c-Ret receptor tyrosine kinase, J. Biol. Chem. 275 (2000) 39159–39166.
[2] H.H. Bock, Y. Jossin, P. Liu, E. Forster, P. May, A.M. Goffinet, J. Herz, Phosphatidylinositol 3-kinase interacts with the adaptor protein Dab1 in response to Reelin signaling and is required for normal cortical lamination, J. Biol. Chem. 278 (2003) 38772–38779.
[3] A. Brunet, S.R. Datta, M.E. Greenberg, Transcription-dependent and -independent control of neuronal survival by the PI3K-Akt signaling pathway, Curr. Opin. Neurobiol. 11 (2001) 297–305.
[4] L.C. Cantley, The phosphoinositide 3-kinase pathway, Science 296 (2002) 1655–1657.
[5] P. Chomczynski, N. Sacchi, Single-step method of RNA isolation by acid guanidinium thiocyanate-phenol-chloroform extraction, Anal. Biochem. 162 (1987) 156–159.
[6] C.Y. Chung, S. Funamoto, R.A. Firtel, Signaling pathways controlling cell polarity and chemotaxis, Trends Biochem. Sci. 26 (2001) 557–566.
[7] F.I. Comer, C.A. Parent, PI 3-kinases and PTEN: how opposites chemoattract, Cell 109 (2002) 541–544.
[8] D.A. Fruman, R.E. Meyers, L.C. Cantley, Phosphoinositide kinases, Annu. Rev. Biochem. 67 (1998) 481–507.
[9] S. Funamoto, R. Meili, S. Lee, L. Parry, R.A. Firtel, Spatial and temporal regulation of 3-phosphoinositides by PI 3-kinase and PTEN mediates chemotaxis, Cell 109 (2002) 611–623.
[10] A. Hall, Rho GTPases and the actin cytoskeleton, Science 279 (1998) 509–514.
[11] H. Hayashi, M. Ichihara, T. Iwashita, H. Murakami, Y. Shimono, K. Kawai, K. Kurokawa, Y. Murakumo, T. Imai, H. Funahashi, A. Nakao, M. Takahashi, Characterization of intracellular signals via tyrosine 1062 in RET activated by glial cell line-derived neurotrophic factor, Oncogene 19 (2000) 4469–4475.

[12] M. Honma, K. Namikawa, K. Mansur, T. Iwata, N. Mori, H. Iizuka, H. Kiyama, Developmental alteration of nerve injury induced glial cell line-derived neurotrophic factor (GDNF) receptor expression is crucial for the determination of injured motoneuron fate, J. Neurochem. 82 (2002) 961–975.
[13] P. Hu, A. Mondino, E.Y. Skolnik, J. Schlessinger, Cloning of a novel, ubiquitously expressed human phosphatidylinositol 3-kinase and identification of its binding site on p85, Mol. Cell. Biol. 13 (1993) 7677–7688.
[14] M. Iijima, P. Devreotes, Tumor suppressor PTEN mediates sensing of chemoattractant gradients, Cell 109 (2002) 599–610.
[15] K. Inukai, M. Anai, E. Van Breda, T. Hosaka, H. Katagiri, M. Funaki, Y. Fukushima, T. Ogihara, Y. Yazaki, M. Kikuchi, Y. Oka, T. Asano, A novel 55-kDa regulatory subunit for phosphatidylinositol 3-kinase structurally similar to p55PIK Is generated by alternative splicing of the p85alpha gene, J. Biol. Chem. 271 (1996) 5317–5320.
[16] K. Inukai, M. Funaki, T. Ogihara, H. Katagiri, A. Kanda, M. Anai, Y. Fukushima, T. Hosaka, M. Suzuki, B.C. Shin, K. Takata, Y. Yazaki, M. Kikuchi, Y. Oka, T. Asano, p85alpha gene generates three isoforms of regulatory subunit for phosphatidylinositol 3-kinase (PI 3-Kinase), p50alpha, p55alpha, and p85alpha, with different PI 3-kinase activity elevating responses to insulin, J. Biol. Chem. 272 (1997) 7873–7882.
[17] K. Inukai, M. Funaki, M. Nawano, H. Katagiri, T. Ogihara, M. Anai, Y. Onishi, H. Sakoda, H. Ono, Y. Fukushima, M. Kikuchi, Y. Oka, T. Asano, The N-terminal 34 residues of the 55 kDa regulatory subunits of phosphoinositide 3-kinase interact with tubulin, Biochem. J. 346 (Pt 2) (2000) 483–489.
[18] K. Inukai, M. Funaki, M. Anai, T. Ogihara, H. Katagiri, Y. Fukushima, H. Sakoda, Y. Onishi, H. Ono, M. Fujishiro, M. Abe, Y. Oka, M. Kikuchi, T. Asano, Five isoforms of the phosphatidylinositol 3-kinase regulatory subunit exhibit different associations with receptor tyrosine kinases and their tyrosine phosphorylations, FEBS Lett. 490 (2001) 32–38.
[19] Y. Ito, H. Sakagami, H. Kondo, Enhanced gene expression for phosphatidylinositol 3-kinase in the hypoglossal motoneurons following axonal crush, Brain Res. Mol. Brain Res. 37 (1996) 329–332.
[20] K. Kimura, S. Hattori, Y. Kabuyama, Y. Shizawa, J. Takayanagi, S. Nakamura, S. Toki, Y. Matsuda, K. Onodera, Y. Fukui, Neurite outgrowth of PC12 cells is suppressed by wortmannin, a specific inhibitor of phosphatidylinositol 3-kinase, J. Biol. Chem. 269 (1994) 18961–18967.
[21] S. Kiryu, N. Morita, K. Ohno, H. Maeno, H. Kiyama, Regulation of mRNA expression involved in Ras and PKA signal pathways during rat hypoglossal nerve regeneration, Brain Res. Mol. Brain Res. 29 (1995) 147–156.
[22] Y. Kita, K.D. Kimura, M. Kobayashi, S. Ihara, K. Kaibuchi, S. Kuroda, M. Ui, H. Iba, H. Konishi, U. Kikkawa, S. Nagata, Y. Fukui, Microinjection of activated phosphatidylinositol-3 kinase induces process outgrowth in rat PC12 cells through the Rac-JNK signal transduction pathway, J. Cell. Sci. 111 (Pt 7) (1998) 907–915.
[23] M. Koltzenburg, P.D. Wall, S.B. McMahon, Does the right side know what the left is doing? Trends Neurosci. 22 (1999) 122–127.
[24] R. Kuruvilla, H. Ye, D.D. Ginty, Spatially and functionally distinct roles of the PI3-K effector pathway during NGF signaling in sympathetic neurons, Neuron 27 (2000) 499–512.
[25] P.C. Letourneau, The cytoskeleton in nerve growth cone motility and axonal pathfinding, Perspect. Dev. Neurobiol. 4 (1996) 111–123.
[26] M. Maeda, N. Ohba, S. Nakagomi, Y. Suzuki, S. Kiryu-Seo, K. Namikawa, W. Kondoh, A. Tanaka, H. Kiyama, Vesicular acetylcholine transporter can be a morphological marker for the reinnervation to muscle of regenerating motor axons, Neurosci. Res. 48 (2004) 305–314.
[27] H.Y. Man, Q. Wang, W.Y. Lu, W. Ju, G. Ahmadian, L. Liu, S. D'Souza, T.P. Wong, C. Taghibiglou, J. Lu, L.E. Becker, L. Pei, F. Liu, M.P. Wymann, J.F. MacDonald, Y.T. Wang, Activation of PI3-kinase is required for AMPA receptor insertion during LTP of mEPSCs in cultured hippocampal neurons, Neuron 38 (2003) 611–624.
[28] K. Namikawa, Q. Su, S. Kiryu-Seo, H. Kiyama, Enhanced expression of 14-3-3 family members in injured motoneurons, Brain Res. Mol. Brain Res. 55 (1998) 315–320.
[29] K. Namikawa, M. Honma, K. Abe, M. Takeda, K. Mansur, T. Obata, A. Miwa, H. Okado, H. Kiyama, Akt/protein kinase B prevents injury-induced motoneuron death and accelerates axonal regeneration, J. Neurosci. 20 (2000) 2875–2886.
[30] Y. Owada, A. Utsunomiya, T. Yoshimoto, H. Kondo, Expression of mRNA for Akt, serine-threonine protein kinase, in the brain during development and its transient enhancement following axotomy of hypoglossal nerve, J. Mol. Neurosci. 9 (1997) 27–33.
[31] S. Sanchez, C.L. Sayas, F. Lim, J. Diaz-Nido, J. Avila, F. Wandosell, The inhibition of phosphatidylinositol-3-kinase induces neurite retraction and activates GSK3, J. Neurochem. 78 (2001) 468–481.
[32] S.H. Shi, L.Y. Jan, Y.N. Jan, Hippocampal neuronal polarity specified by spatially localized mPar3/mPar6 and PI 3-kinase activity, Cell 112 (2003) 63–75.
[33] B.C. Shin, M. Suzuki, K. Inukai, M. Anai, T. Asano, K. Takata, Multiple isoforms of the regulatory subunit for phosphatidylinositol 3-kinase (PI3-kinase) are expressed in neurons in the rat brain, Biochem. Biophys. Res. Commun. 246 (1998) 313–319.
[34] L.R. Stephens, K.T. Hughes, R.F. Irvine, Pathway of phosphatidylinositol(3,4,5)-trisphosphate synthesis in activated neutrophils, Nature 351 (1991) 33–39.
[35] K. Tanabe, S. Kiryu-Seo, T. Nakamura, N. Mori, H. Tsujino, T. Ochi, H. Kiyama, Alternative expression of Shc family members in nerve-injured motoneurons, Brain Res. Mol. Brain Res. 53 (1998) 291–296.
[36] M. Trupp, N. Belluardo, H. Funakoshi, C.F. Ibanez, Complementary and overlapping expression of glial cell line-derived neurotrophic factor (GDNF), c-ret proto-oncogene, and GDNF receptor-alpha indicates multiple mechanisms of trophic actions in the adult rat CNS, J. Neurosci. 17 (1997) 3554–3567.
[37] K. Ueki, P. Algenstaedt, F. Mauvais-Jarvis, C.R. Kahn, Positive and negative regulation of phosphoinositide 3-kinase-dependent signaling pathways by three different gene products of the p85alpha regulatory subunit, Mol. Cell. Biol. 20 (2000) 8035–8046.
[38] K. Ueki, D.A. Fruman, C.M. Yballe, M. Fasshauer, J. Klein, T. Asano, L.C. Cantley, C.R. Kahn, Positive and negative roles of p85 alpha and p85 beta regulatory subunits of phosphoinositide 3-kinase in insulin signaling, J. Biol. Chem. 278 (2003) 48453–48466.
[39] B. Vanhaesebroeck, S.J. Leevers, G. Panayotou, M.D. Waterfield, Phosphoinositide 3-kinases: a conserved family of signal transducers, Trends Biochem. Sci. 22 (1997) 267–272.
[40] F. Wang, P. Herzmark, O.D. Weiner, S. Srinivasan, G. Servant, H.R. Bourne, Lipid products of PI(3)Ks maintain persistent cell polarity and directed motility in neutrophils, Nat. Cell Biol. 4 (2002) 513–518.
[41] O.D. Weiner, P.O. Neilsen, G.D. Prestwich, M.W. Kirschner, L.C. Cantley, H.R. Bourne, A PtdInsP(3)- and Rho GTPase-mediated positive feedback loop regulates neutrophil polarity, Nat. Cell Biol. 4 (2002) 509–513.
[42] M. Whitman, C.P. Downes, M. Keeler, T. Keller, L. Cantley, Type I phosphatidylinositol kinase makes a novel inositol phospholipid, phosphatidylinositol-3-phosphate, Nature 332 (1988) 644–646.
[43] G.L. Yao, H. Kato, M. Khalil, S. Kiryu, H. Kiyama, Selective upregulation of cytokine receptor subchain and their intracellular signalling molecules after peripheral nerve injury, Eur. J. Neurosci. 9 (1997) 1047–1054.
[44] R.D. York, D.C. Molliver, S.S. Grewal, P.E. Stenberg, E.W. McCleskey, P.J. Stork, Role of phosphoinositide 3-kinase and endocytosis in nerve growth factor-induced extracellular signal-regulated kinase activation via Ras and Rap1, Mol. Cell. Biol. 20 (2000) 8069–8083.
[45] Y. Zhang, D.B. Moheban, B.R. Conway, A. Bhattacharyya, R.A. Segal, Cell surface Trk receptors mediate NGF-induced survival while internalized receptors regulate NGF-induced differentiation, J. Neurosci. 20 (2000) 5671–5678.

Dissipating Excess Energy Stored in the Liver Is a Potential Treatment Strategy for Diabetes Associated With Obesity

Yasushi Ishigaki,[1] Hideki Katagiri,[2] Tetsuya Yamada,[1] Takehide Ogihara,[2] Junta Imai,[1,2] Kenji Uno,[1,2] Yutaka Hasegawa,[1,2] Junhong Gao,[1,2] Hisamitsu Ishihara,[1] Tooru Shimosegawa,[3] Hideyuki Sakoda,[4] Tomoichiro Asano,[4] and Yoshitomo Oka[1]

For examining whether dissipating excess energy in the liver is a possible therapeutic approach to high-fat diet–induced metabolic disorders, uncoupling protein-1 (UCP1) was expressed in murine liver using adenoviral vectors in mice with high-fat diet–induced diabetes and obesity, and in standard diet–fed lean mice. Once diabetes with obesity developed, hepatic UCP1 expression increased energy expenditure, decreased body weight, and reduced fat in the liver and adipose tissues, resulting in markedly improved insulin resistance and, thus, diabetes and dyslipidemia. Decreased expressions of enzymes for lipid synthesis and glucose production and activation of AMP-activated kinase in the liver seem to contribute to these improvements. Hepatic UCP1 expression also reversed high-fat diet–induced hyperphagia and hypothalamic leptin resistance, as well as insulin resistance in muscle. In contrast, intriguingly, in standard diet–fed lean mice, hepatic UCP1 expression did not significantly affect energy expenditure or hepatic ATP contents. Furthermore, no alterations in blood glucose levels, body weight, or adiposity were observed. These findings suggest that ectopic UCP1 in the liver dissipates surplus energy without affecting required energy and exerts minimal metabolic effects in lean mice. Thus, enhanced UCP expression in the liver is a new potential therapeutic target for the metabolic syndrome. *Diabetes* 54:322–332, 2005

From the [1]Division of Molecular Metabolism and Diabetes, Tohoku University Graduate School of Medicine, Sendai, Japan; the [2]Division of Advanced Therapeutics for Metabolic Diseases, Center for Translational and Advanced Animal Research, Tohoku University Graduate School of Medicine, Sendai, Japan; the [3]Division of Gastroenterology, Tohoku University Graduate School of Medicine, Sendai, Japan; and the [4]Department of Internal Medicine, Faculty of Medicine, University of Tokyo, Tokyo, Japan.

Address correspondence and reprint requests to Hideki Katagiri, MD, PhD, Division of Advanced Therapeutics for Metabolic Diseases, Center for Translational and Advanced Animal Research, Tohoku University Graduate School of Medicine, 2-1 Seiryo-machi, Aoba-ku, Sendai 980-8575, Japan. E-mail: katagiri-tky@umin.ac.jp.

Received for publication 19 April 2004 and accepted in revised form 13 October 2004.

Y.I., H.K., and T.Y. contributed equally to this work.

ACC1, acetyl-CoA carboxylase 1; AMPK, AMP-activated protein kinase; CPT1, carnitine palmitoyltransferase 1; IRS1, insulin receptor substrate 1; PPAR, peroxisome proliferator–activated receptor; SREBP, sterol regulatory element binding protein; TNF-α, tumor necrosis factor-α; UCP, uncoupling protein.

An explosive increase in the number of diabetic patients, which has become a major public health concern in most industrialized countries in recent decades (1), is mainly the result of excess energy intake and physical inactivity. When food intake chronically exceeds metabolic needs, efficient metabolism causes excess energy storage and results in obesity, a common condition associated with diabetes, hyperlipidemia, and premature heart disease. Excess energy in cells lowers the response to insulin, namely insulin resistance. However, the major treatment modalities for diabetes, including insulin injection and oral sulfonylureas, aim at lowering blood glucose levels by driving glucose into cells in peripheral tissues such as muscle and fat. This further exacerbates insulin resistance when energy intake is in excess, resulting in a vicious cycle. Therefore, novel therapies that promote increased energy expenditure are needed.

Inefficient metabolism, such as the generation of heat instead of ATP, is a potential treatment strategy for type 2 diabetes associated with obesity. Uncoupling proteins (UCPs) were discovered members of the mitochondrial inner membrane carrier family. These proteins leak protons into the mitochondrial matrix, dissipating energy as heat rather than allowing it to be captured in ATP (2). UCP1 (thermogenin) was originally identified in brown adipose tissue and demonstrated to mediate nonshivering thermogenesis. UCP1 plays an important role in mediating cold exposure–induced thermogenesis (3) and is also a likely regulator of diet-induced thermogenesis (4).

Several laboratories have reported overexpression of UCPs, using the transgenic approach, in mice (5–8). These reports indicate that overexpression of UCPs in white adipose tissue and skeletal muscle has preventive effects on development of genetic and dietary obesity and the resultant insulin resistance. However, it is still unclear whether ectopic UCP1 expression exerts therapeutic effects after the development of diabetes associated with obesity.

The liver is one of the major metabolic organs involved in glucose and lipid metabolism and insulin action. In addition, the liver can store and release abundant fat

TABLE 1
Sequences of quantitative RT-PCR primers

Probe	Primer 1	Primer 2
FAS	5'-tgctcccagctgcaggc-3'	5'-gcccggtagctctgggtgta-3'
SCD-1	5'-tgggttggctgcttgtg-3'	5'-gcgtgggcaggatgaag-3'
SREBP1c	5'-catggattgcacatttgaag-3'	5'-cctgtgtcccctgtctca-3'
FAT	5'-tggctaaatgagactgggacc-3'	5'- acatcaccactccaatcccaag-3'
MCAD	5'-tcgaaagcggctcacaagcag-3'	5'-caccgcagctttccggaatgt-3'
UCP2	5'-cattctgaccatggtgcgtactga-3'	5'-gttcatgtatctcgtcttgaccac-3'
PPAR-α	5'-ggatgtcacacaatgcaattcgc-3'	5'-tcacagaacggcttcctcaggt-3'
PEPCK	5'-agcggatatggtgggaac-3'	5'-ggtctccactccttgttc-3'
G6Pase	5'-aaagagactgtgggcatcaatc-3'	5'-aatgcctgacaagactccagcc-3'
GAPDH	5'-accacagtccatgccatcac-3'	5'-tccaccaccctgttgctgta-3'

FAS, fatty acid synthase; SCD1, stearoyl-CoA desaturase 1; FAT, fatty acid transporter; MCAD, medium-chain acyl-CoA dehydrogenase; PEPCK, phosphoenolpyruvate carboxylase; G6Pase, glucose-6-phosphatase; GAPDH, glyceraldehyde-3-dehydrogenase.

dynamically, in response to the energy balance. We reported that hepatic AKT activation resulted in marked alterations in glucose and lipid metabolism (9), suggesting that the liver is a potential site of ectopic expression. We herein expressed UCP1 protein in the liver, before or after diabetes associated with dietary obesity had developed. We found that hepatic UCP1 expression improved diabetes and obesity under high-fat diet conditions through local effects in the liver as well as remote effects in adipose tissues, muscle, and the hypothalamus. However, in standard diet–fed lean mice, effects on glucose and lipid metabolism were minimal. Using gene transduction after disease development, as in this study, provides useful information allowing analysis of therapeutic, rather than preventive, effects that would be difficult to examine using congenitally gene-engineered animal models.

RESEARCH DESIGN AND METHODS

Preparation of recombinant adenovirus. Murine UCP1 cDNA (10) was provided by Professor Leslie P. Kozak (Pennington Biomedical Research Center). Murine liver carnitine palmitoyltransferase 1 (CPT1a) cDNA was obtained by RT-PCR with liver total RNA and primers designed from the reported sequence (GenBank accession no. NM_013495). Recombinant adenovirus, containing murine UCP1 (11) or CPT1a cDNA under the CAG promoter, was prepared as described previously (12). A recombinant adenovirus bearing the bacterial β-galactosidase gene (*Adex1CAlacZ*) (13) was used as a control.

Animals. Animal studies were conducted under protocols in accordance with the institutional guidelines for animal experiments at Tohoku University. Male C57BL/6N mice were housed individually and divided into high-fat diet (32% safflower oil, 33.1% casein, 17.6% sucrose, and 5.6% cellulose [14]) and standard diet (65% carbohydrate, 4% fat, and 24% protein) groups at 5 weeks of age, when body weights were 21.2 ± 0.25 g (means ± SE). Four weeks after separation, body weight–matched mice for each group received an injection of adenovirus via the tail vein. Viruses were administered intravenously at a dose of 2×10^8 plaque-forming units. For pair-feeding experiments, after 4 weeks of high-fat diet, mice were allotted into three groups. Two groups of mice received an injection of UCP1 or LacZ adenovirus. After 24 h, mice in the third group received an injection of LacZ adenovirus. The latter LacZ mice were given their daily food allotments on the basis of the previous day's consumption by UCP1 mice.

Antibodies. UCP1, acetyl-CoA carboxylase 1 (ACC 1), and insulin receptor antibodies were purchased from Santa Cruz Biotechnology (Santa Cruz, CA). The α-subunit of AMP-activated protein kinase (AMPK), phospho-AMPK (Thr172), and phospho-ACC (Ser79) antibodies were purchased from Cell Signaling Technology (Beverly, MA). Affinity-purified antibody against insulin receptor substrate 1 (IRS1) was prepared as described previously (15).

Immunoblotting. Tissue samples were prepared as previously described (9), and tissue protein extracts (250 μg of total protein) were boiled in Laemmli buffer that contained 10 mmol/l dithiothreitol and subjected to SDS-PAGE. The immunoblots were visualized with an enhanced chemiluminescence detection kit (Amersham, Buckinghamshire, U.K.).

Triglyceride content of the liver. Frozen livers were homogenized, and triglycerides were extracted with $CHCl_3$:CH_3OH (2:1, vol:vol), dried, and resuspended in 2-propanol (16). Triglyceride contents were measured using Lipidos liquid (TOYOBO, Osaka, Japan).

Oxygen consumption. Oxygen consumption was measured with an O_2/CO_2 metabolism measuring system (model MK-5000RQ; Muromachikikai, Tokyo, Japan). Each mouse was kept unrestrained in a sealed chamber with an air flow of 0.5 l/min for 5 h at 25°C without food or water during the light cycle. Air was sampled every 3 min, and the consumed oxygen concentration (Vo_2) was calculated.

Histological analysis. Livers as well as epididymal fat (white adipose tissue) and brown adipose tissues were removed and fixed with 10% formalin and embedded in paraffin. Tissue sections were stained with hematoxylin and eosin. Total adipocyte areas were traced manually and analyzed. Brown and white adipocyte areas were measured in 100 or more cells per mouse in each group.

Measurement of body temperature. Rectal temperature was measured with a Thermalert TH-5 (Physitemp, Clifton, NJ).

Measurement of ATP. The ATP levels in liver homogenates were measured with a luciferase-luciferin system (17) by using an ATP determination kit (Molecular Probes, Eugene, OR).

Measurement of AMPK activity. Livers were homogenized, and aliquots of supernatant were incubated with anti-AMPK α-subunit antibody. AMPK activity in the immunoprecipitates was assessed as a function of SAMS peptide phosphorylation, as previously described (18).

Tyrosine phosphorylation of insulin receptor and IRS1. Mice that were fasted for 16 h received an injection of 100 μl of normal saline (0.9% NaCl), with or without 10 units/kg body wt insulin, via the tail vein. Hindlimb muscles were removed 300 s later and immediately homogenated. After centrifugation, the resultant supernatants were used for immunoprecipitation with anti–insulin receptor or anti-IRS1 antibody. Immunoprecipitates were subjected to SDS-PAGE and then immunoblotted using anti-phosphotyrosine antibody (4G10) or individual antibodies as described previously (15).

Blood analysis. Blood glucose was assayed with Antsense II (Horiba Industry, Kyoto, Japan). Serum insulin and leptin were determined with ELISA kits (Morinaga Institute of Biological Science, Yokohama, Japan). Serum adiponectin and tumor necrosis factor-α (TNF-α) concentrations were measured with an ELISA kit (Ohtsuka Pharmaceutical, Tokyo, Japan) and a TNF-α assay kit (Amersham Biosciences, Uppsala, Sweden), respectively. Serum total cholesterol, triglyceride, and free fatty acid concentrations were determined with a Cholescolor liquid, Lipidos liquid (TOYOBO), and NEFA C (Wako Pure Chemical, Osaka, Japan) kits, respectively.

Glucose, insulin, and leptin tolerance tests. Glucose tolerance tests were performed on fasted (10 h) mice. Mice were given oral glucose (2 g/kg body wt), and blood glucose was assayed immediately before and at 15, 30, 60, and 120 min after administration. Insulin tolerance tests were performed on fed mice. Mice received an injection of human regular insulin (0.75 units/kg body wt; Eli Lilly, Kobe, Japan) into the intraperitoneal space, and blood glucose was assayed immediately before and at 20, 40, 60, and 80 min after injection. Leptin tolerance tests were performed as reported previously (19) with slight modification. Fasted (12 h) mice received an injection of mouse leptin (7.2 mg/kg body wt; R&D Systems) into the intraperitoneal space, and food intake amounts for 12 h thereafter were determined. Ratios of food intake amounts to those of vehicle-injected mice were calculated.

Quantitative RT-PCR–based gene expression. Total RNA was isolated from 0.1 g of mouse hepatic tissue with ISOGEN (Wako Pure Chemical), and

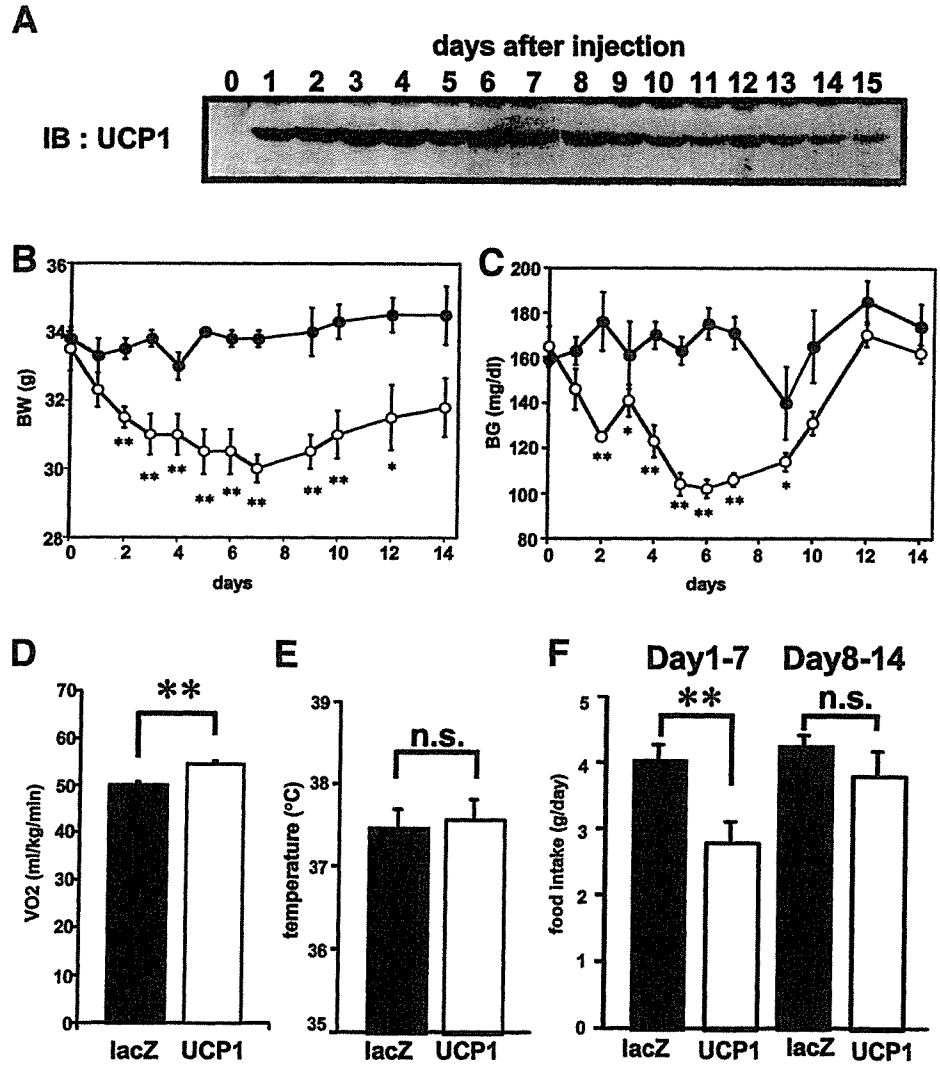

FIG. 1. Hepatic UCP1 expression reduced body weight and blood glucose levels. *A*: Ectopic UCP1 expression in the liver in high-fat–fed mice was detected by immunoblotting of hepatic extracts (250 μg total protein/lane). Liver samples were collected at different times after adenovirus injection. *B* and *C*: Body weights (*B*) and blood glucose levels (*C*) in the ad libitum–fed state after adenoviral administration in control (LacZ) mice (●) and UCP1 mice (○; $n = 4$ per group). *D*: Resting Vo_2 was measured on day 3 after adenoviral injection with open-circuit indirect calorimetry. All mice were kept in a cage for ~5 h in the daytime without food or water ($n = 5$ per group). *E*: Rectal temperature was measured in the ad libitum–fed state on day 7 after adenoviral injection ($n = 6$ per group). *F*: Average daily food intake amounts over the first and the second weeks after adenoviral administration are presented. Regarding all panels, similar results were obtained from 10 or more experiments, and representative results are presented as means ± SE. *$P < 0.05$, **$P < 0.01$ assessed by unpaired t test.

cDNA synthesis was performed with a Cloned AMV First Strand Synthesis Kit (Invitrogen, Rockville, MD) using 5 μg of total RNA. cDNA synthesized from total RNA was evaluated in a real-time PCR quantitative system (Light Cycler Quick System 350S; Roche Diagnostics, Mannheim, Germany). The relative amount of mRNA was calculated with glyceraldehyde-3-dehydrogenase mRNA as the invariant control. The primers used are described in Table 1.

All data were expressed as means ± SE. The statistical significance of differences was assessed by the unpaired t test and one-factor ANOVA.

RESULTS

Hepatic UCP1 expression increased energy expenditure and reduced body weight and blood glucose levels in mice that had high-fat diet–induced obesity and diabetes. C57BL/6 mice were on a high-fat diet for 4 weeks, resulting in diabetes associated with obesity. The UCP1 adenovirus vector (11) was then administered intravenously (UCP1 mice). Mice that were given the LacZ adenovirus were used as a control (LacZ mice). No significant alterations were observed in body weights (Fig. 1*B*), blood glucose levels (Fig. 1*C*), food intake amounts, body temperature, or plasma lipid parameters (data not shown) before versus after LacZ adenovirus administration. Systemic infusion of recombinant adenoviruses into mice through the tail vein primarily resulted in expression of transgenes in the liver, with no detectable expression in peripheral tissues such as muscle, fat, kidney, or brain (data not shown), as reported previously (20). As shown in Fig. 1*A*, immunoblotting revealed that ectopic UCP1 expression in the liver peaked on day 3. Maximal expression was maintained through day 8. After day 9, hepatic expression of UCP1 decreased, and very small amounts of UCP1 protein were detected on day 14 (Fig. 1*A*).

In UCP1 mice, body weight and blood glucose levels were markedly decreased (Fig. 1*B* and *C*) concomitantly with hepatic expression levels of UCP1. On day 7, body weights of UCP1 mice were significantly lower, by 13%, than those of control mice. After day 9, body weight and

blood glucose levels began to increase as the expression of hepatic UCP1 declined. These findings indicate that hepatic UCP1 expression exerted therapeutic effects on diabetes associated with diet-induced obesity.

Resting oxygen consumption on day 3 was markedly increased, by 12%, in UCP1 mice compared with controls (Fig. 1*D*), whereas rectal temperature did not differ between the two (Fig. 1*E*). Thus, ectopic UCP1 in the liver, like endogenous UCP1 in brown adipocytes, promoted inefficient metabolism, thereby enhancing energy expenditure and leading to weight reduction. This effect, however, was not sufficient to raise whole-body temperature. In addition, hepatic UCP1 expression changed food intake. Whereas without hepatic UCP1 expression, food intake amounts in high-fat–fed mice were markedly increased compared with those in standard diet–fed lean mice (compare Figs. 1*F* and 5*D*), hepatic UCP1 expression reversed hyperphagia in mice with high-fat diet–induced obesity and diabetes (Fig. 1*F*). After day 8, concomitantly with the drop in hepatic UCP1 expression, hyperphagia was restored (Fig. 1*F*). In contrast, mice received an intravenous injection of adenovirus encoding CPT1a, another mitochondrial protein, did not show significantly altered food consumption (data not shown), suggesting that food intake suppression induced by hepatic UCP1 expression is not a nonspecific effect of expression of any of the hepatic mitochondrial proteins.

To eliminate any secondary effects of reduced food intake induced by hepatic UCP1 expression, we performed pair-feeding experiments. In contrast to UCP1 mice, pair-fed LacZ mice exhibited only slight decreases in body weights and blood glucose levels (of 3.1 and 6.9%, respectively, on day 7 after adenoviral administration). These results suggest that increased energy expenditure is an important mechanism underlying marked improvements of obesity and diabetes in UCP1 mice.

Hepatic UCP1 expression decreased fat contents in the liver and adipose tissues. Hepatic and adipose fat accumulations were examined on day 7 after adenoviral gene delivery. In the high-fat–fed control mice, liver weight and triglyceride content were markedly increased compared with the standard chow–fed lean mice (compare Fig. 2*A* and *B* with Fig. 5*E* and *F*, respectively). Hepatic UCP1 expression significantly decreased liver weight (Fig. 2*A*) and triglyceride content (Fig. 2*B*) compared with LacZ mice, with high-fat feeding. It is interesting that hepatic UCP1 expression also decreased fat content in their adipose tissues. For example, epididymal fat weight was significantly decreased in UCP1 mice compared with that in controls (Fig. 2*C*). Thus, hepatic expression of UCP1 exerts not only local effects in the liver but also remote effects on metabolism in other tissues.

These results were confirmed by the histological findings. No apparent infiltration or structural change was observed in the livers of either LacZ mice or UCP1 mice, indicating the absence of adenovirus-induced liver damage (Fig. 2*D*). Whereas abundant lipid droplets were present in the livers of control mice, these lipid droplets were markedly diminished in UCP1 mouse livers, indicating marked improvement of fatty liver findings in response to UCP1 expression (Fig. 2*D*). Furthermore, the cell diameters in epididymal fat (Fig. 2*E*) and brown adipose (Fig. 2*F*) tissues were significantly decreased in UCP1 mice. Expression levels of endogenous UCP1 protein in brown adipocytes were similar in the two groups (Fig. 2*G*), suggesting that energy expenditure in brown adipocytes was not increased in UCP1 mice. These findings suggest that hepatic UCP1 expression promotes hydrolysis of triglycerides already stored in adipose tissues, leading to smaller adipocytes with the resultant fatty acids being mobilized and metabolized as a substrate for oxidation in the liver.

Hepatic expressions of enzymes involved in lipid metabolism and glucose production. To elucidate the underlying mechanism whereby stored fat was decreased in the liver by hepatic UCP1 expression, we examined the expressions of proteins involved in lipid metabolism by quantitative RT-PCR. Significant reductions in the expressions of the lipogenic enzymes, including stearoyl-CoA desaturase-1 and fatty acid synthase, were observed in UCP1 mice (Fig. 3*A*). Sterol regulatory element binding protein 1c (SREBP1c) expression in the liver tended to be diminished. In contrast, hepatic expressions of enzymes involved in fatty acid oxidation tended to be increased. In particular, expressions of fatty acid transporter and UCP2 were significantly increased (Fig. 3*B*).

We further examined expression levels of key enzymes for hepatic glucose production. Hepatic phosphoenolpyruvate carboxykinase and glucose-6-phosphatase expressions were significantly decreased in UCP1 mice (Fig. 3*C*), suggesting a decrease to contribute to improvement of diabetes.

UCP1 expression may activate AMPK as a result of decreased generation of ATP. AMPK activation reportedly decreases malonyl-CoA generation via inhibition of ACC (21), resulting in enhancement of fatty acid oxidation. Therefore, ATP levels and AMPK phosphorylation in the liver were examined in LacZ and UCP1 mice under ad libitum feeding conditions. Hepatic ATP concentrations in UCP1 mice were approximately half those in control mice (Fig. 3*D*) but still ~2.3-fold those in standard diet–fed control mice. Hepatic AMPK activity was increased 1.6-fold in UCP1 mice compared with LacZ mice (Fig. 3*E*). The phosphorylation state of the α-subunit of AMPK in the liver was enhanced in UCP1 mice (Fig. 3*F*). Furthermore, resultant enhancement of hepatic ACC phosphorylation was observed (Fig. 3*G*). These findings suggest that AMPK activation induced by UCP1 expression plays an important role in the observed marked improvement of fatty liver findings via enhanced fatty acid oxidation.

Glucose and lipid metabolism in UCP1 mice. The results of oral glucose tolerance (Fig. 4*A*) and insulin tolerance (Fig. 4*B*) tests on day 7 after adenoviral administration clearly showed that hepatic expression of UCP1 markedly improved glucose tolerance and insulin sensitivity in obese and diabetic mice. Improved insulin sensitivity in muscle was confirmed by enhanced insulin receptor and IRS1 phosphorylation (Fig. 4*C*) in response to insulin administration. Thus, hepatic UCP1 expression exerts a remote beneficial effect on insulin sensitivity in muscle.

In addition, plasma lipid parameters were decreased in UCP1 mice. Total plasma cholesterol levels tended to be decreased in UCP1 mice compared with controls, although the changes were not statistically significant (Fig. 4*D*). Plasma triglyceride and free fatty acid levels were signifi-